Cell Reports

Article

Antibodies targeting the shared cytokine receptor IL-1 receptor accessory protein invoke distinct mechanisms to block all cytokine signaling

Graphical abstract

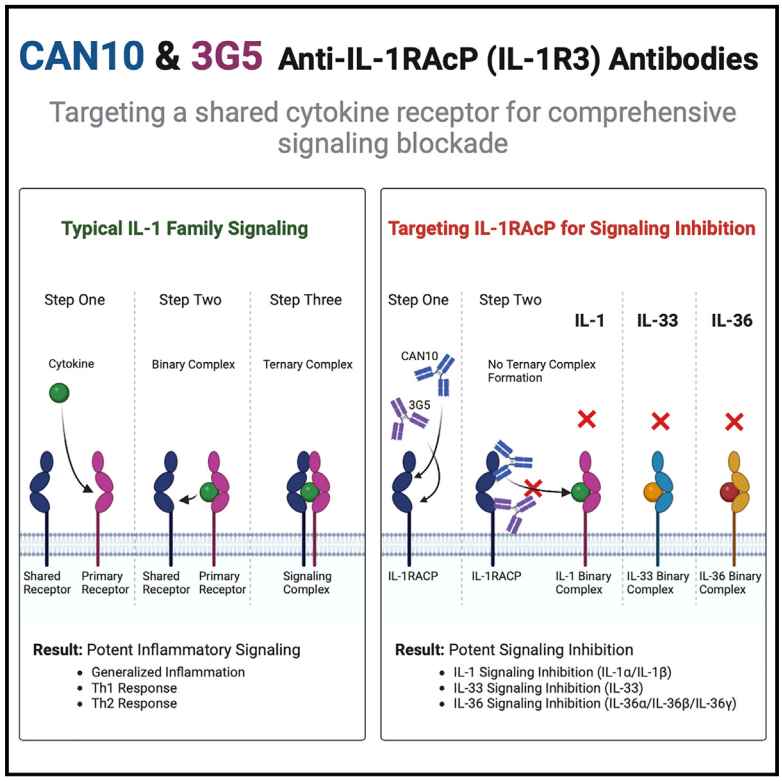

Highlights

- Two mAbs specific for IL-1RAcP block all IL-1, IL-33, and IL-36 signaling
- CAN10 and 3G5 block signaling with similar potency but through distinct mechanisms
- Blocking all IL-1RAcP cytokines is better than solely IL-1 in a mouse model
- Shared receptors are viable therapeutic targets; CAN10 is in clinical trials

Authors

James K. Fields, Elin Jaensson Gyllenbäck, Marek Bogacz, ..., David Liberg, Daniel Deredge, Eric J. Sundberg

Correspondence

eric.sundberg@emory.edu

In brief

Fields et al. demonstrate the viability of targeting a shared cytokine receptor for comprehensive signaling blockade of all associated cytokines. CAN10 and 3G5, two anti-IL-1RAcP antibodies, target distinct epitopes on this shared receptor and potently block IL-1α, IL-1β, IL-33, IL-36α, IL-36β, and IL-36γ signaling.

Fields et al., 2024, Cell Reports *43*, 114099
May 28, 2024
https://doi.org/10.1016/j.celrep.2024.114099

CellPress

Cell Reports

CellPress
OPEN ACCESS

Article

Antibodies targeting the shared cytokine receptor IL-1 receptor accessory protein invoke distinct mechanisms to block all cytokine signaling

James K. Fields,[1,2,6] Elin Jaensson Gyllenbäck,[3] Marek Bogacz,[1] Juliet Obi,[2] Gabriel Svensson Birkedal,[3] Kjell Sjöström,[4] Kino Maravillas,[1] Caitríona Grönberg,[3] Sara Rattik,[3] Kyle Kihn,[2] Maria Flowers,[1] Ally K. Smith,[2] Nils Hansen,[5] Thoas Fioretos,[5] Chau Huyhn,[1] David Liberg,[3] Daniel Deredge,[2] and Eric J. Sundberg[1,7,*]

[1]Department of Biochemistry, Emory University School of Medicine, Atlanta, GA 30322, USA
[2]Department of Pharmaceutical Sciences, University of Maryland School of Pharmacy, Baltimore, MD 21201, USA
[3]Cantargia AB, Lund, Sweden
[4]Innovagen AB, Lund, Sweden
[5]Division of Clinical Genetics, Department of Laboratory Medicine, Lund University, Lund, Sweden
[6]Present address: Department of Biophysics and Biophysical Chemistry, Johns Hopkins School of Medicine, Baltimore, MD 21205, USA
[7]Lead contact
*Correspondence: eric.sundberg@emory.edu
https://doi.org/10.1016/j.celrep.2024.114099

SUMMARY

Interleukin-1 (IL-1)-family cytokines are potent modulators of inflammation, coordinating a vast array of immunological responses across innate and adaptive immune systems. Dysregulated IL-1-family cytokine signaling, however, is involved in a multitude of adverse health effects, such as chronic inflammatory conditions, autoimmune diseases, and cancer. Within the IL-1 family of cytokines, six—IL-1α, IL-1β, IL-33, IL-36α, IL-36β, and IL-36γ—require the IL-1 receptor accessory protein (IL-1RAcP) as their shared co-receptor. Common features of cytokine signaling include redundancy of signaling pathways, sharing of cytokines and receptors, pleiotropy of the cytokines themselves, and multifaceted immune responses. Accordingly, targeting multiple cytokines simultaneously is an emerging therapeutic strategy and can provide advantages over targeting a single cytokine pathway. Here, we show that two monoclonal antibodies, CAN10 and 3G5, which target IL-1RAcP for broad blockade of all associated cytokines, do so through distinct mechanisms and provide therapeutic opportunities for the treatment of inflammatory diseases.

INTRODUCTION

Cytokines are messengers of the immune system. These small, soluble proteins function at vanishingly low concentrations to elicit myriad immune responses across the breadth of human immunity, often in response to external stimuli. While essential to fighting disease and maintaining tissue homeostasis, dysregulated cytokine signaling contributes to a multitude of harmful outcomes, including inflammatory conditions, autoimmune diseases, and cancer. Importantly, inhibiting signaling from these inflammatory molecules can lead to a reduction or reversal of many of the associated diseases, such as with interleukin-1 (IL-1), tumor necrosis factor alpha, and IL-6-blocking therapies.[1–15]

Common features associated with cytokine signaling include the redundancy of the signaling pathways, the sharing of receptors and ligands, the pleiotropy of the cytokines themselves, and the multifaceted immune responses that occur as a result of their action.[16] Indeed, a properly functioning immune system is an intricate dance of signals in which the molecules involved orchestrate a concerted response. Dysregulation of these signals, however, can quickly induce a cascade of inflammation or immunosuppression. To effectively target many inflammatory and autoimmune diseases, it may be necessary to block multiple immune signals simultaneously.

IL-1 family cytokines represent a prime example of such interwoven signals. The IL-1 superfamily is composed of seven agonistic cytokines, four inhibitory cytokines, and 10 receptors.[17,18] Among this group, six cytokines, IL-1α (also called IL-1F1), IL-1β (IL-1F2), IL-33 (IL-1F11), IL-36α (IL-1F6), IL-36β (IL-1F8), and IL-36γ (IL-1F9), share the IL-1 receptor accessory protein (IL-1RAcP [IL-1R3]) as their common co-receptor; the remaining IL-1-family agonist cytokine, IL-18 (IL-1F4), utilizes its own distinct co-receptor, IL-18 receptor beta (IL-18Rβ [IL-1R7]). IL-1 family signaling occurs in a stepwise process, with a cytokine binding to its cognate, or private, receptor at high (nanomolar to sub-nanomolar) affinity (IL-1RI for IL-1α and IL-1β, ST2 [IL-1R4] for IL-33, and IL-36R [IL-1R6] for IL-36α, IL-36β, and IL-36γ). Next, the shared, or public, co-receptor IL-1RAcP is recruited to form a signaling-competent ternary complex, utilizing four conserved regions on IL-1RAcP: the c2d2 loop and the hydrophobic patch on domain 2, the linker between

domain 2 (D2) and domain 3 (D3), and molecular surfaces on D3.[19,20] As these cytokine/receptor/co-receptor complexes form, cytoplasmic Toll/IL-1 receptor (TIR) domains, connected to each of the receptor and co-receptor ectodomains via single transmembrane α helices, oligomerize to initiate a potent MyD88-dependent signaling cascade.[19]

Targeting the shared co-receptor IL-1RAcP therapeutically has emerged as a putative treatment for different types of solid cancers. The forerunner of this strategy is CAN04, also known as nadunolimab.[20] CAN04, a monoclonal human immunoglobulin G (IgG), is enhanced for antibody-dependent cellular cytotoxicity by Fc engineering and thus able to function through both signaling blockade and by targeting IL-1RAcP-expressing tumor cells for immune mediated killing. CAN04 is being studied clinically in combination with chemotherapy for the treatment of pancreatic cancer and non-small cell lung cancer (ClinicalTrials.gov: NCT03267316) as well as triple-negative breast cancer (ClinicalTrials.gov: NCT05181462). Since IL-1 signaling is implicated in tumor chemoresistance, downregulation of IL-1 signaling, in addition to tumor targeting, may provide a synergistic anti-tumor effect with chemotherapy beyond anti-IL1RAP monotherapy alone.[21] Hematological cancers may also be a very relevant target area, since IL-1RAcP overexpression has been found to be a biomarker for acute myeloid leukemia (AML) and chronic myeloid leukemias (CML).[22–24] Prior to these findings, no cell-surface markers existed to distinguish CML from normal hematopoietic stem cells.[22] Notably, in AML and CML, downregulating inflammatory IL-1 signaling, in addition to targeting the shared receptor IL-1RAcP, also indicated an augmented benefit of the treatment.[24,25]

In addition to IL-1RAcP being a potential target in different cancers, simultaneous blockade of IL-1RAcP-dependent pathways could also be beneficial in a wide range of inflammatory and fibrotic diseases. Notably, IL-1RAcP-associated cytokine signaling can drive a multitude of immunological responses, such as generalized inflammation, a Th1 response, or a Th2 response.[26–29] In addition to their many functions, IL-1RAcP-associated cytokines have prominent roles in barrier immunity and, often, there is redundancy of cytokine usage, such as IL-1 and IL-36 in epithelial and mucosal immunity.[30] Unsurprisingly, this dual signaling is seen in disease states as well, such as the concerted roles of IL-1 and IL-36 in psoriasis or IL-1 and IL-33 in asthma, tissue remodeling, and chronic obstructive pulmonary disease.[31–43] Thus, to inhibit multiple inflammatory signals simultaneously, IL-1RAcP is a prime target for monoclonal antibody (mAb) therapy.[44,45] Indeed, initial studies have revealed the ability of an antibody against IL-1RAcP to alleviate monosodium urate (MSU) crystal-mediated peritonitis, ovalbumin-induced allergic airway inflammation, and imiquimod-induced psoriasis *in vivo* through broad signaling blockade.[44]

Here, we identify two mAbs, CAN10 and 3G5, as potent blockers of IL-1RAcP-dependent signaling by IL-1, IL-33, and IL-36 cytokines. Hence, CAN10, which has entered phase 1 clinical trials (ClinicalTrials.gov: NCT06143371), and 3G5 represent candidates for IL-1RAcP targeting in inflammatory diseases. Furthermore, we describe the molecular mechanisms of IL-1RAcP-dependent signaling blockade by these two anti-IL-1RAcP mAbs and show that CAN10 and 3G5 bind entirely unique, non-overlapping epitopes on the IL-1RAcP molecular surface and, thereby, utilize different strategies to block IL-1 cytokine signaling. Despite the distinct mechanisms of IL-1 family cytokine signaling inhibition by these two mAbs, their inhibitory capacities for all IL-1RAcP-dependent cytokines are nearly identical and therefore provide two viable therapeutic strategies for targeting a shared receptor for broad signaling blockade.

RESULTS

Targeting the shared co-receptor IL-1RAcP is a potent therapeutic strategy that outperforms IL-1 blockade alone

To emphasize the therapeutic benefit of blocking the inflammatory signaling of multiple IL-1-family cytokines *in vivo,* we employed a mouse model that utilizes MSU crystals to induce acute peritonitis, a model of human disease dependent on NLRP3 inflammasome activation.[46] Here, upon administration of MSU, a marked influx of innate immune cells into the peritoneal cavity of IL-1RAcP wild-type (WT) mice was observed, with neutrophils dominating the cellular landscape (Figure 1A). In the context of an IL-1RAcP knockout mouse, we did not observe this rapid influx of innate immune cells, establishing the importance of the shared receptor IL-1RAcP in mediating this disease state (Figure 1A).

To further investigate the benefits of blocking IL-1RAcP compared to IL-1 signaling alone, we utilized an mAb specific to murine IL-1RAcP (mIL-1RAcP): mCAN10 (Figure S1A). While the exact epitope of mCAN10 is unknown, and consideration should be taken in any direct comparisons to CAN10, its binding to IL-1RAcP has been localized to D2 through the generation of mouse/human chimeras of IL-1RAcP (Figure S1B). This antibody was developed as a functional surrogate anti-mIL-1RAcP antibody, as it potently blocks all mIL-1RAcP-associated cytokines (Figures S1C–S1H). To test this strategy, either the anti-mIL-1RAcP antibody mCAN10, an isotype control antibody, or an equimolar concentration of the natural IL-1 receptor antagonist (IL-1Ra) was administered to mice prior to administration of MSU (Figure 1B). As expected, prior treatment with either mCAN10 or IL-1Ra significantly decreased peritoneal cavity-infiltrating leukocytes, in particular neutrophils, thus displaying the contribution of IL-1 signaling to this disease state (Figure 1C). Furthermore, while both mCAN10 and IL-1Ra decreased IL-6 and G-CSF compared to their controls, mCAN10 had a more potent effect on IL-6 and also reduced eotaxin, IL-5, MCP-1, and MIP-1b (Figure 1D). Together, these data indicate that, despite the clear IL-1-dependent effects in this model, additional inflammatory molecules present can be blocked by the inhibition of IL-1RAcP, in agreement with Hojen et al.[44] Furthermore, we expand upon these earlier findings by the inclusion of an IL-1RAcP knockout animal, demonstrating the importance of the shared receptor to this disease state, as well as the inclusion of the chemokine eotaxin and the cytokine IL-5, molecules integral to eosinophil migration, maturation, and activation.[47,48] Altogether, the targeting of IL-1RAcP and, therefore, blocking of all associated cytokines had a greater effect than solely blocking IL-1 alone in this disease model (Figures 1C and 1D).

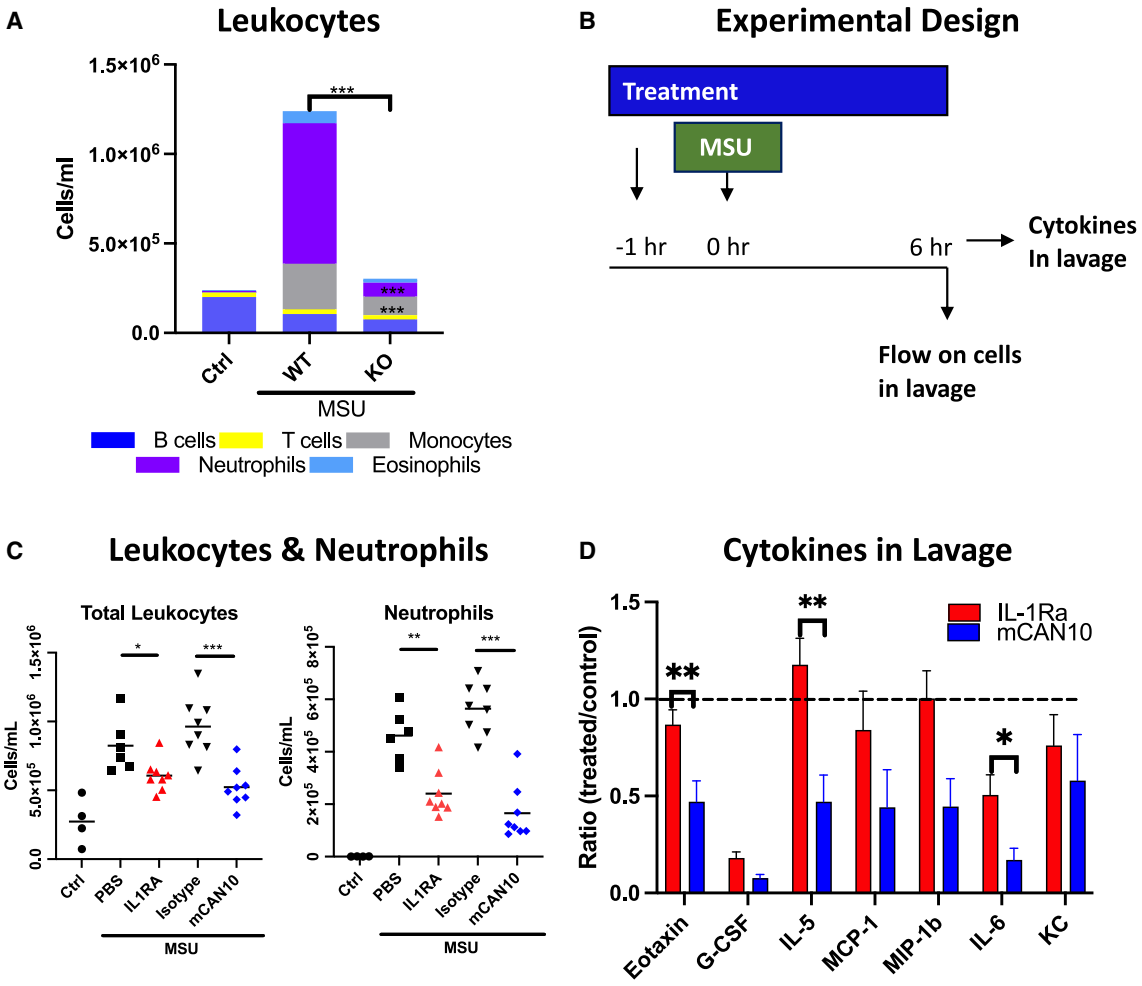

Figure 1. IL-1RAcP blockade decreases monosodium urate (MSU) crystal-induced inflammation in an acute peritonitis model more potently than IL-1Ra treatment alone

(A) Cellular landscape of peritoneal lavage with no MSU exposure and after MSU exposure 6 h post in IL-1RAcP WT (n = 11) and knockout (KO) (n = 6) mice. The graph shows mean values.

(B–D) Experimental design (B) for the MSU experiment with administration of control (PBS), IL-1Ra, mIgG2a isotype control, or anti-IL-1RAcP antibody (mCAN10).

(C) Leukocyte and neutrophil concentrations by flow cytometry in peritoneal lavage fluid after 6 h after MSU administration. The line is at the mean. Each symbol represents one mouse.

(D) Cytokine profiles by Luminex from peritoneal lavage of IL-1Ra and anti-IL-1RAcP antibody mCAN10 treatments, normalized to vehicle and isotype controls, respectively. The graph shows mean and SEM.

Statistical analysis was done using Mann-Whitney *$p < 0.05$, **$p < 0.01$, ***$p < 0.005$, ****$p < 0.001$. In (A), the statistics above the bars show differences for total cells per milliliter, while the statistics inside the bars show differences for neutrophils and monocytes specifically. In (D), statistics are shown for mCAN10 vs. IL1Ra normalized to their vehicle and isotype controls (iso), respectively. Statistics not shown: decrease in concentrations of analytes for IL1Ra and mCAN10 vs. their respective controls; G-CSF (IL1Ra vs. PBS ***, mCAN10 vs. iso ***), IL-6 (IL1Ra vs. PBS **, mCAN10 vs. iso **), IL-5 (IL1Ra vs. PBS ns; mCAN10 vs. iso *), eotaxin (IL1Ra vs. PBS ns, mCAN10 vs. iso **), MIP1b (IL1Ra vs. PBS ns, mCAN10 vs. iso *), MCP1 (IL1Ra vs. PBS ns, mCAN10 vs. iso *), KC (Keratinocyte Chemoattractant/CXCL1) (IL1Ra vs. PBS ns, mCAN10 vs. iso ns).

CAN10 and 3G5 block signaling of all six IL-1RAcP-associated cytokines

Next, we investigated antibodies against human IL-1RAcP. As IL-1RAcP is the shared co-receptor for six different agonist cytokines, we tested the abilities of CAN10 and 3G5 to block these cytokines from initiating their potent signaling cascades in comparison to their natural antagonists (Figures 2A and 2B). IL-1RI, ST2, and IL-1RAcP, the primary and co-receptors for IL-1α, IL-1β, and IL-33, are expressed in HEK-Blue IL-1/IL-33 cells, and, thus, these cells were used to assess the ability of CAN10 and 3G5 to inhibit IL-1α and IL-1β signaling (Figures 2C and 2D). Here, recombinant IL-1Ra inhibited IL-1α the most potently, with an IC_{50} of 23 pM (Figure 2C). Both CAN10 and 3G5 also inhibited IL-1α potently, albeit less than IL-1Ra, with IC_{50} values of 416 pM and 878 pM, respectively. In IL-1β signaling, IL-1Ra displayed an IC_{50} of 109 pM, while CAN10 displayed an IC_{50} of 650 pM and 3G5 an IC_{50} of 1.43 nM (Figure 2D).

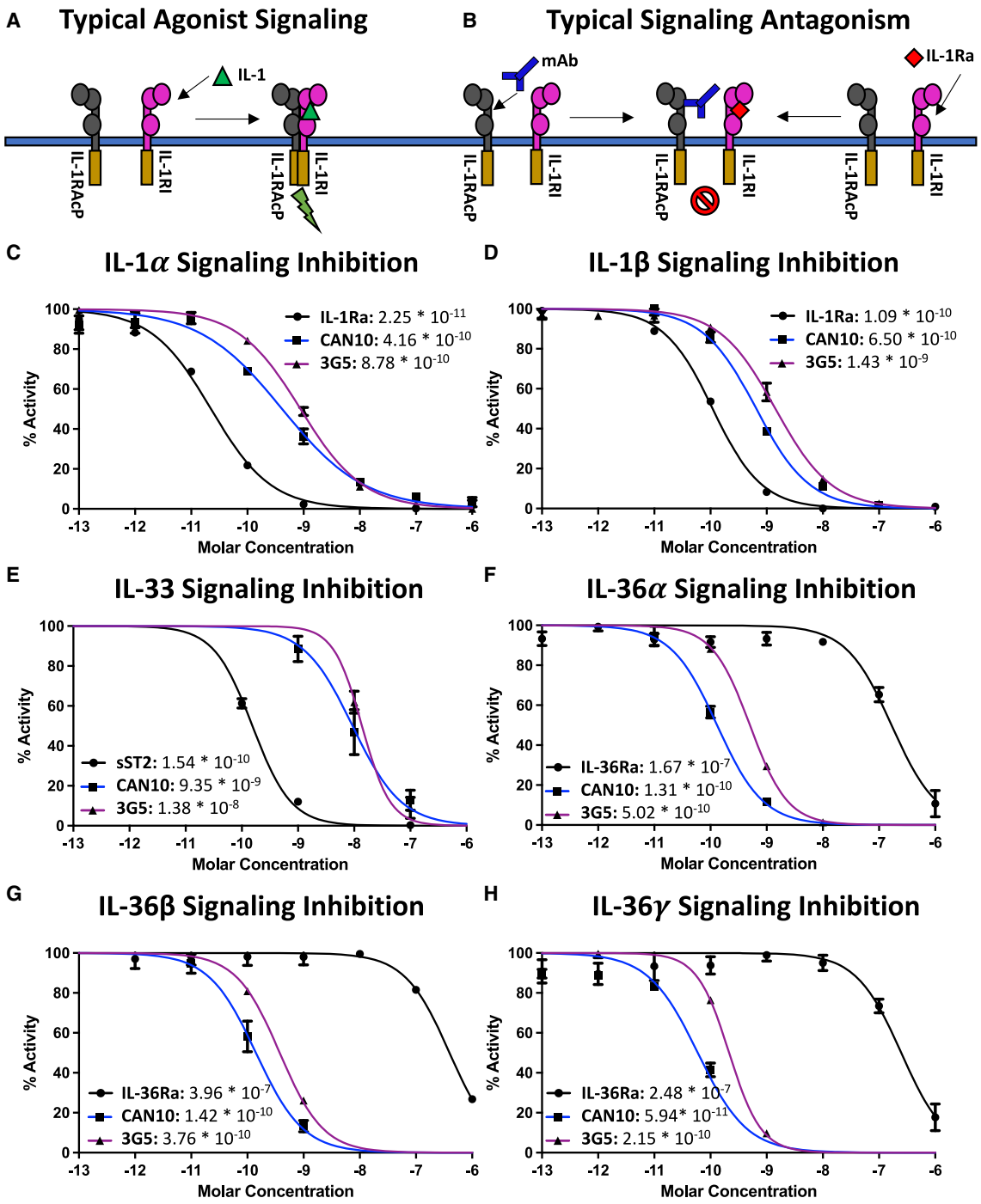

Figure 2. Cell signaling assays for all IL-1RAcP-associated cytokines

(A) A cartoon of typical IL-1-family agonist signaling, demonstrating the cytokine IL-1 binding its primary receptor IL-1RI and recruiting the shared secondary receptor IL-1RAcP to form a signaling-competent ternary complex (i.e., cytokine/primary receptor/secondary receptor).

(B) A cartoon of typical IL-1-family signaling antagonism, demonstrating the natural antagonist IL-1Ra binding to the primary receptor IL-1RI and precluding the recruitment of IL-1RAcP to form a signaling-competent ternary complex. In addition, a monoclonal antibody (mAb) is shown binding to IL-1RAcP and precluding the formation of a signaling-competent ternary complex.

(C) Cell signaling assays of IL-1α with the natural antagonist IL-1Ra, the antibody CAN10, and the antibody 3G5 with error bars denoting SEM.

(D) Cell signaling assays of IL-1β with the natural antagonist IL-1Ra, the antibody CAN10, and the antibody 3G5 with error bars denoting SEM.

(legend continued on next page)

Next, we tested IL-33, a Th2-associated cytokine that also utilizes IL-1RAcP as its co-receptor, for signaling inhibition by CAN10 and 3G5. Unlike the IL-1 and IL-36 cytokines, IL-33 is located on a different chromosome and does not have an antagonist cytokine to inhibit its action.[49] Instead, IL-33 utilizes a soluble spliced isoform of its primary receptor ST2, soluble ST2 (sST2), as a form of signaling inhibition.[50,51] sST2 was the most potent IL-33 inhibitor, with an IC_{50} of 154 pM, while CAN10 and 3G5 inhibited IL-33 signaling nearly 100-fold less than sST2, with IC_{50} values of 9.35 nM and 14 nM, respectively (Figure 2E).

IL-36 cytokines include three isoforms, IL-36α, IL-36β, and IL-36γ, and are associated with a generalized Th1 response.[28] As with IL-1 signaling, there exists an antagonist cytokine, IL-36Ra, that acts as a negative regulator of IL-36 signaling.[52] In IL-36α signaling, CAN10 and 3G5 were both potent inhibitors, displaying IC_{50} values of 131 pM and 502 pM, respectively, while IL-36Ra displayed an approximately 1,000-fold weaker IC_{50} of 167 nM (Figure 2F). In IL-36β signaling, CAN10 and 3G5 displayed IC_{50} values of 142 pM and 376 pM, respectively, while IL-36Ra was again nearly 1,000-fold weaker at an IC_{50} of 396 nM (Figure 2G). In IL-36γ signaling, both CAN10 and 3G5 were the most potent inhibitors, displaying IC_{50} values of 59 pM and 215 pM, respectively, while IL-36Ra displayed an IC_{50} of 248 nM (Figure 2H). In conclusion, CAN10 and 3G5 inhibited all IL-1RAcP-associated cytokines, with IL-1- and IL-36-associated cytokines being inhibited the most potently as compared to their natural antagonists. Indeed, even when tested with all six cytokines simultaneously, CAN10 and 3G5 were able to potently inhibit all IL-1RAcP-associated inflammatory signaling (Figure S2A).

CAN10 and 3G5 both bind with high affinity to IL-1RAcP but to distinct domains

The biological consequence of an antibody-antigen interaction is highly dependent on both the duration and location of antibody binding. To determine the binding parameters of the antibodies CAN10 and 3G5 to their common antigen IL-1RAcP, we conducted surface plasmon resonance (SPR) analysis (Figure 3). Both CAN10 and 3G5 bound with high affinity to IL-1RAcP, with similar K_D values of 167 pM and 141 pM, respectively (Figures 3A and 3B). These high affinities translated to fast on-rates and slow off-rates for both antibodies. CAN10 displayed an on-rate of 9.4×10^5 (1/ms) and an off-rate of 1.57×10^{-4} (1/s); 3G5 displayed an on-rate of 1.59×10^6 (1/ms) and an off-rate of 2.25×10^{-4} (1/s). As IL-1RAcP is heavily glycosylated, with seven putative glycosylation sites, we sought to determine whether glycans played a role in binding for either antibody by using a deglycosylated form of IL-1RAcP as the antigen (Figure S2B). Neither CAN10 nor 3G5 were affected by this change in glycosylation, with both antibodies displaying similar affinities, 183 pM and 80 pM, respectively, for their deglycosylated IL-1RAcP antigen (Figures 3C and 3D).

To determine which regions of IL-1RAcP contained the binding epitopes of CAN10 and 3G5, we produced two fragments of the IL-1RAcP ectodomain and tested binding of these mAbs to each of these IL-1RAcP fragments (Figure S2B). The IL-1RAcP ectodomain is composed of three Ig domains, D1–D3, from N to C termini. D1 and D2 form a stable complex with an inter-domain interface of 762 $Å^2$, while D3 is tethered to D2 by a flexible linker. In IL-1-family signaling, cytokine/cognate receptor complexes utilize molecular surfaces from both D2 and D3 to form ternary signaling complexes.[53,54,55] By analogous SPR analysis as for full-length IL-1RAcP ectodomains, we observed that CAN10 bound D1/D2 with an affinity of 119 pM, nearly identical to the full-length IL-1RAcP, but did not bind to D3 (Figures 3E and 3G). Conversely, 3G5 did not bind D1/D2 but bound D3 with an affinity of 118 pM, likewise similar to its affinity to the full-length IL-1RAcP ectodomain (Figures 3F and 3H). Together, these data indicate that CAN10 and 3G5 bind different domains of IL-1RAcP and that binding to the respective domain is sufficient to account for the binding affinity to the full-length IL-1RAcP.

CAN10 and 3G5 recognize distinct IL-1RAcP epitopes

To assess the contribution of different epitopes of IL-1RAcP to CAN10 binding, we took advantage of the inability of CAN10 to bind murine IL-1RAcP and generated chimeric constructs of IL-1RAcP (Figure S3). Utilizing the murine IL-1RAcP (mIL-1RAcP) backbone, we combined different stretches of human IL-1RAcP (hIL-1RAcP) that covered the main areas where human and murine sequences deviate on D2 of IL-1RAcP (Figures S3A and S3B). To this end, we generated the following two chimeric proteins: H1, inclusive of residues Pro121–Arg137, and H2, inclusive of residues Thr154–Ile171, an area covering the entire c2d2 loop and part of the hydrophobic patch. Using these chimeric variants, we observed restored binding to mIL-1RAcP by CAN10 only when the H2 sequence was present (Figure S3C).

To further define the binding epitopes and molecular mechanisms of IL-1 family cytokine signaling inhibition by CAN10 and 3G5, we next employed hydrogen-deuterium exchange mass spectrometry (HDX-MS; Figures S4A and S4B). We found that CAN10 bound IL-1RAcP on a highly localized region on D2, covered by the H2 sequence identified above and corresponding to the c2d2 loop, residues Q165–N169, notable for its high energetic contributions for known signaling complex formation (Figure 4A).[54] This change in deuterium uptake occurred along five main peptide fragments, individually comprising residues W157–F167, Y162–N176, Y162–L177, Y162–F179, and Y162–L180 (Figures 4B and S4C). Three peptide fragments, N168–N176, N168–F179, and N168–L180, where we observed no difference in deuterium uptake at the first two time points, allowed us to further localize binding to preceding peptide stretches (Figures 4B and S4C). This precise targeting of the c2d2 loop by CAN10 was reflected by the antibodies' discrete CDR usage (Figure 4C). We conclude that CAN10 utilizes four adjacent CDRs

(E) Cell signaling assays of IL-33 with the natural antagonist sST2, the antibody CAN10, and the antibody 3G5 with error bars denoting SEM.
(F) Cell signaling assays of IL-36α with the natural antagonist IL-36Ra, the antibody CAN10, and the antibody 3G5 with error bars denoting SEM.
(G) Cell signaling assays of IL-36β with the natural antagonist IL-36Ra, the antibody CAN10, and the antibody 3G5 with error bars denoting SEM.
(H) Cell signaling assays of IL-36γ with the natural antagonist IL-36Ra, the antibody CAN10, and the antibody 3G5 with error bars denoting SEM.

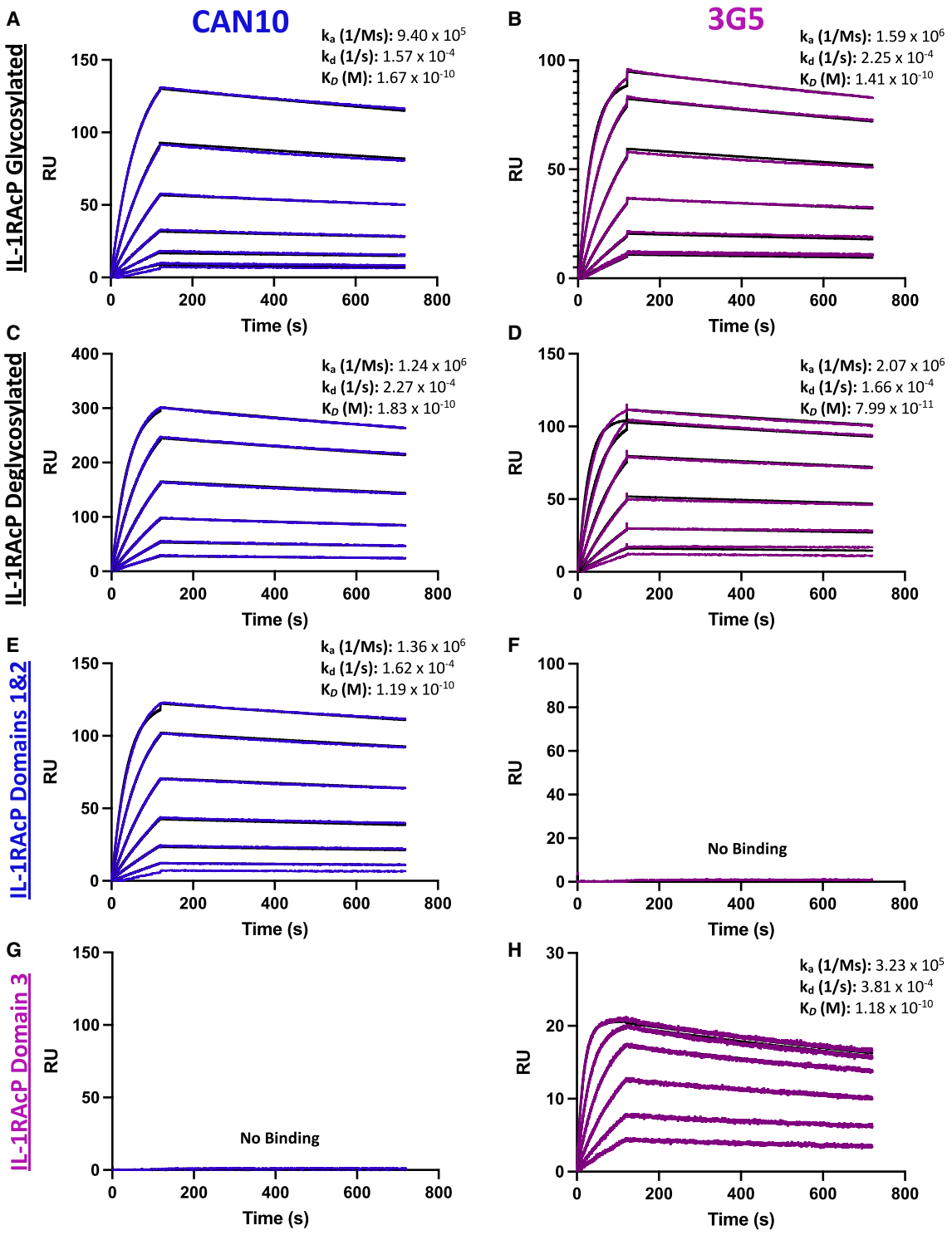

Figure 3. SPR of the antibodies CAN10 and 3G5 to IL-1RAcP

(A) Sensorgram (black) with fit (blue) of CAN10 with IL-1RAcP as the antigen, with the k_a, k_d, and K_D of the interaction labeled.

(B) Sensorgram (black) with fit (purple) of 3G5 with IL-1RAcP as the antigen, with the k_a, k_d, and K_D of the interaction labeled.

(C) Sensorgram (black) with fit (blue) of CAN10 with deglycosylated IL-1RAcP as the antigen with the k_a, k_d, and K_D of the interaction labeled.

(D) Sensorgram (black) with fit (purple) of 3G5 with deglycosylated IL-1RAcP as the antigen, with the k_a, k_d, and K_D of the interaction labeled.

(legend continued on next page)

for its interaction with IL-1RacP, including the light-chain CDR2 and heavy-chain CDR1, CDR2, and CDR3 (Figures 4D and S4D).

Unlike CAN10, 3G5 bound IL-1RacP on its D3 in two main regions (Figure 5A). We observed the highest protection on peptides P222–Y234, P222–E241, and P223–Y234, residues shown previously to be important for IL-33 signaling (Figures 5B and S5A).[54] Additionally, we observed IL-1RAcP protection imparted by 3G5 on peptides V276–D289, V276–T293 V276–L296, and I278–I298 (Figures 5B and S5A), which correspond to residues found previously to be important for IL-1 signaling.[53,54] This large interface is further reflected in the broad paratope of 3G5, wherein the antibody utilizes five of its six CDRs (Figure 5C), including light-chain CDR1, CDR2, and CDR3 as well as heavy-chain CDR2 and CDR3 (Figures 5D and S5B).

Fine specificity of CAN10 and 3G5 antibodies defined by alanine scanning mutagenesis

From our signaling inhibition assays, chimeric IL-1RAcP receptors, and HDX-MS experiments, we found that CAN10 and 3G5 block IL-1RAcP-associated cytokine signaling and bound regions required by all known IL-1-family cytokines. To define the fine specificity of these mAbs for IL-1RAcP, we employed an alanine scanning mutagenesis library of individual interfacial residues utilized in known IL-1-family signaling complexes (Figure 6A).[54,45]

Notably, CAN10 again bound most prominently to IL-1RAcP residues that form the c2d2 loop in our alanine scan (Figures 6A and 6B). The F167A mutation resulted in the largest energetic change in CAN10 binding, exhibiting a ΔΔG of more than 3 kcal/mol. Adjacent to this residue, the N166A mutation resulted in a ΔΔG of over 2 kcal/mol binding energy, and N168A resulted in an approximately 1.75 kcal/mol change in binding free energy (Figures 6A and S6A; Table S1). Other mutations in this region of the IL-1RAcP surface that resulted in significant ΔΔG values included I171A at nearly 1 kcal/mol and M159 at 0.45 kcal/mol. 3G5 displayed no significant changes in binding to mutations in either the c2d2 loop or the hydrophobic patch, a finding consistent with both our SPR and HDX-MS data.

3G5 bound in a highly localized region of the IL-1RAcP D3 (Figure 6B). This included changes in binding free energy of 1.3 kcal/mol for V224A, 2.4 kcal/mol for H226A, and 1.85 kcal/mol for Y249A (Figures 6A and S7A; Table S2). Smaller changes in energetic contributions were seen in more distal locations of D3, including 0.3 kcal/mol for the R286A mutation, which resides in a region known to be important for IL-1 signaling.[54] CAN10 displayed no significant changes in binding to mutations in D3, in agreement with our SPR and HDX-MS data.

Due to the high degree of specificity of these antibodies to regions utilized in known signaling complexes, we investigated whether these antibodies could act synergistically. Indeed, through our biophysical characterization of CAN10 and 3G5, we observed clear evidence of distinct, distant epitopes on IL-1RAcP. These findings were further strengthened by our simultaneous binding experiments, wherein CAN10 could bind IL-1RAcP in the presence of 3G5 and vice versa (Figures S8A and S8B). CAN10 and 3G5, however, did not inhibit IL-1 signaling in a synergistic manner, suggesting that their precise targeting on IL-1RAcP is the peak of signaling inhibition for antibodies targeting this shared receptor (Figure S8C).

DISCUSSION

Inflammatory signaling has long been known as a double-edged sword in human immunity. While integral to a functioning immune system, aberrant inflammatory signaling can lead to a multitude of adverse health conditions. Dysregulated IL-1 family cytokines are central mediators of acute and chronic inflammation, and the role of IL-1 in cancer has been well established.[56–59] As with other cytokine families, such as the type I and type II classes of cytokines, the IL-1 family utilizes shared receptors within many of its signaling complexes.[19,60] Our studies confirm the increased potency of targeting IL-1RAcP to reduce inflammation compared to IL-1 blockade alone and describe the mechanism by which the two anti-IL-1RAcP mAbs, CAN10 and 3G5, block all IL-1-family cytokines that utilize this shared co-receptor.

To date, all known IL-1-family ternary complexes that utilize IL-1RAcP as a shared receptor are grossly similar.[53,54,55] Structurally, a β-trefoil cytokine binds a primary receptor composed of three Ig domains, thereby recruiting a co-receptor of similar architecture to form a ternary signaling complex (Figures 7A and 7B).[19] Between the IL-1β and IL-33 signaling-competent ternary complexes, there exists a difference of only 3.2Å root-mean-square deviation (RMSD) over their C-α atoms, highlighting the similarity of these ternary complex structures (Figures 7A and 7B).[53,54]

Despite these similarities, IL-1β and IL-33 use distinct strategies in their recruitment of IL-1RAcP. IL-1β signaling utilizes D2 of IL-1RAcP as the energetic driver of its interaction with the cytokine/receptor pair IL-1β/IL-1RI.[54] This is due primarily to the interactions of the cytokine's β 11/12 loop with the c2d2 loop of IL-1RAcP, with N166 of IL-1RAcP contributing 1 kcal/mol, F167 of IL-1RAcP 4 kcal/mol, and N169 of IL-1RAcP nearly 4.5 kcal/mol to IL-1β complex formation (Figure 7C).[53,54,55] Indeed, the interaction between IL-1β and the c2d2 loop of IL-1RAcP is so important that a β 11/12 loop swap of IL-1Ra onto IL-1β diminishes IL-1β/IL-1RI binding to IL-1RAcP 40-fold; conversely, a β 11/12 and β 4/5 loop swap of IL-1β onto the antagonist cytokine IL-1Ra almost entirely restores binding of IL-1RAcP by the antagonist binary complex (IL-1Ra/IL-1RI) to a level comparable with IL-1 β/IL-1RI recruitment, hypothetically reversing the antagonist function of IL-1Ra.[55] Although there are no high-resolution structures to date of an IL-36 signaling complex (i.e., IL-36/IL-36R/IL-1RAcP), initial structural investigations into IL-36 signaling have demonstrated

(E) Sensorgram (black) with fit (blue) of CAN10 with D1 and D2 of IL-1RAcP as the antigen, with the k_a, k_d, and K_D of the interaction labeled.
(F) Sensorgram (purple) of 3G5 with D1 and D2 of IL-1RAcP as the antigen.
(G) Sensorgram (blue) of CAN10 with D3 of IL-1RAcP as the antigen.
(H) Sensorgram (black) with fit (purple) of 3G5 with D3 of IL-1RAcP as the antigen, with the k_a, k_d, and K_D of the interaction labeled.

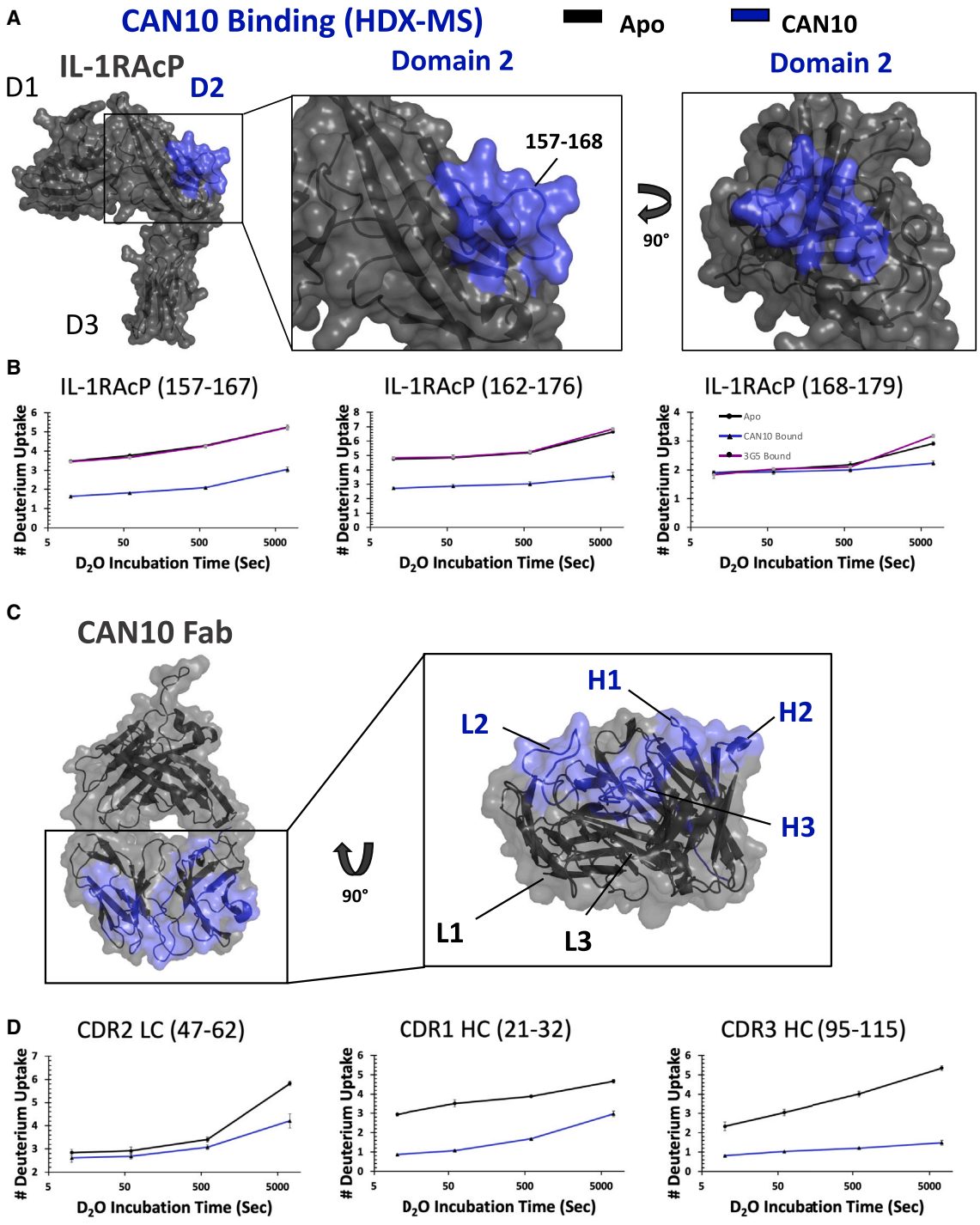

Figure 4. Deuterium exchange protection on IL-1RAcP by the antibody CAN10

(A) Crystal structure of IL-1RAcP (PDB: 4DEP) with CAN10 HDX-MS binding colored blue. D2 is enlarged to show peptides involved in CAN10 binding from both front and side views.

(B) Peptide stretches identified by HDX-MS for CAN10 deuterium exchange differences between Apo IL-1RAcP (black), CAN10-bound IL-1RAcP (blue), and 3G5-bound IL-1RAcP (purple) with error bars denoting standard deviation.

(C) Model of Fab CAN10 with IL-1RAcP HDX-MS binding colored blue.

(D) Peptide stretches identified by HDX-MS for CAN10 deuterium exchange differences between Apo CAN10 (black) and IL-1RAcP-bound CAN10 (blue) with error bars denoting standard deviation.

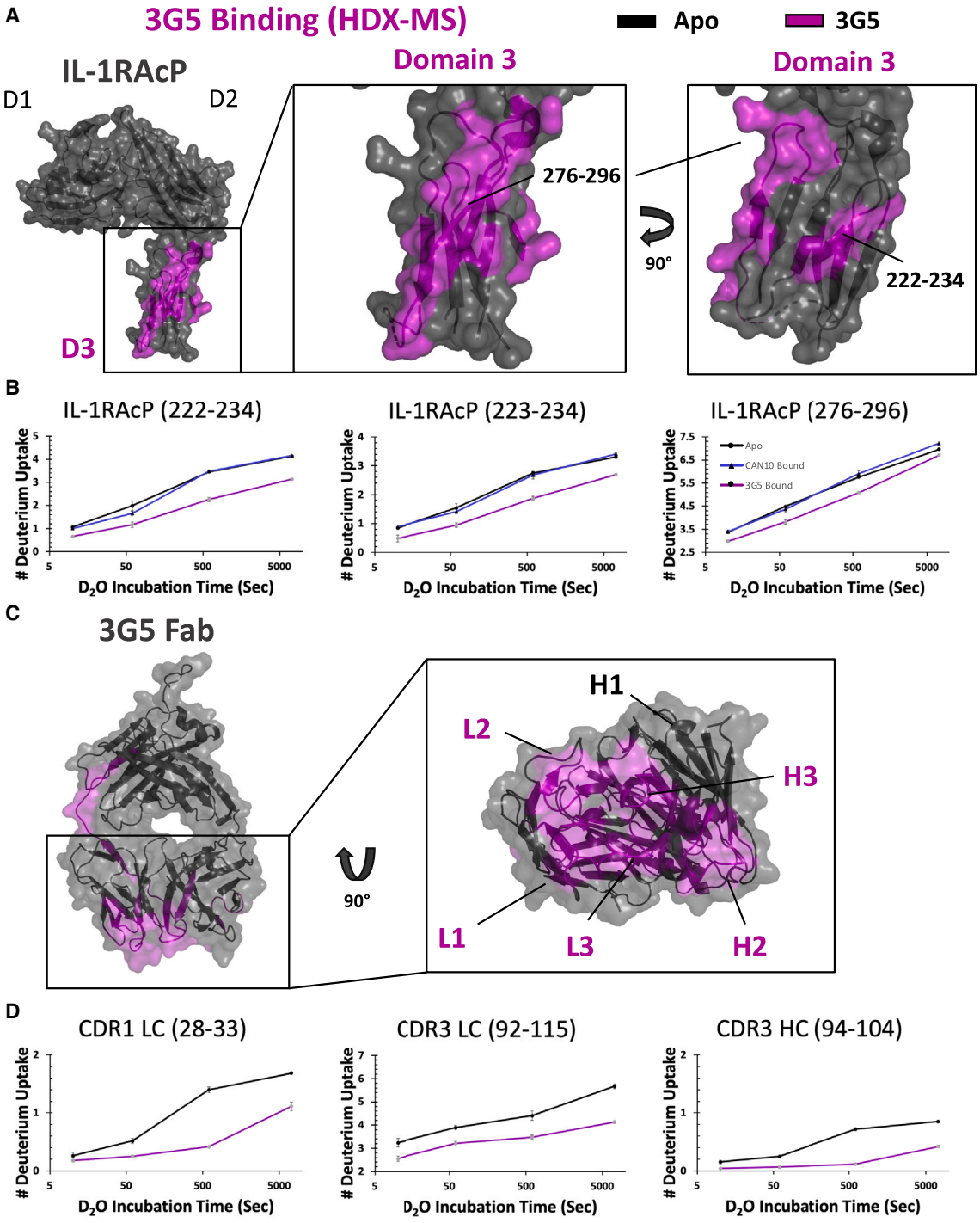

Figure 5. Deuterium exchange protection on IL-1RAcP by the antibody 3G5

(A) Crystal structure of IL-1RAcP (PDB: 4DEP), with 3G5 HDX-MS binding colored purple. D3 is enlarged to show peptides involved in 3G5 binding from both front and side views.

(B) Peptide stretches identified by HDX-MS for 3G5 deuterium exchange differences between Apo IL-1RAcP, CAN10-bound IL-1RAcP, and 3G5-bound IL-1RAcP with error bars denoting standard deviation.

(C) Crystal structure of Fab 3G5 (PDB: 8VFU) with IL-1RAcP HDX-MS binding colored purple.

(D) Peptide stretches identified by HDX-MS for 3G5 deuterium exchange differences between Apo 3G5 (black) and IL-1RAcP-bound 3G5 (purple) with error bars denoting standard deviation.

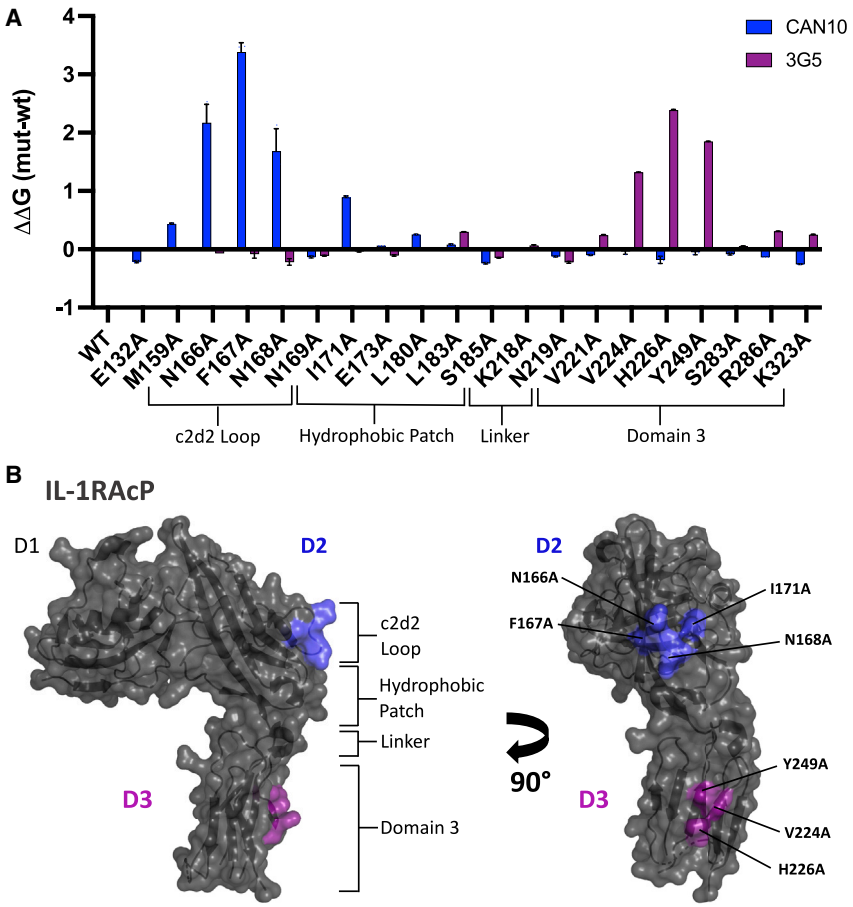

Figure 6. IL-1RAcP SPR alanine scan of interfacial residues for CAN10 and 3G5 Fab binding

(A) Graph of energetic contributions (ΔΔG) of each mutation mapped by color of the analyte (Fab), with CAN10 colored blue and 3G5 colored purple with error bars denoting standard deviation. Peptides on the x axis are labeled according to their location on the c2d2 loop, hydrophobic patch, linker, or D3.

(B) IL-1RAcP (PDB: 4DEP) with CAN10 binding (blue) and 3G5 (purple) colored according to alanine scan data. IL-1RAcP residues and ternary complex interfacial binding areas of IL-1RAcP are labeled.

that IL-36Ra antagonism works similarly to IL-1Ra antagonism.[61] In short, IL-36Ra antagonism functions in part by disrupting interactions in the c2d2 loop of IL-1RAcP through steric clashes in IL-36Ra's extended β 11/12 loop.[61] Indeed, loop swaps of the β 11/12 from IL-36Ra into IL-36γ resulted in a 14-fold decrease in affinity of IL-36/IL-36R to IL-1RAcP, resulting in an overall 1,000-fold reduction in signaling activity.[61] Consequentially, the c2d2 loop region can be inferred to be an integral component of IL-36 complex formation as well.

If IL-1β signaling could be said to be "cytokine driven," then IL-33 signaling is "receptor driven," with the cytokine IL-33 holding its primary receptor ST2 in a conformation amenable to IL-1RAcP recruitment rather than the cytokine making extensive contacts with IL-1RAcP (Figure 7D).[54] While the c2d2 loop of IL-1RAcP remains an important and prominent interface for IL-33 signaling within D2, with N166, F167, N168 of IL-1RAcP individually contributing nearly 1 kcal/mol and N169 of IL-1RAcP contributing over 2 kcal/mol to IL-33 complex formation, the binding interface between IL-1RAcP and the IL-33/ST2 binary complex is distributed almost equally between D2 and D3 of IL-1RAcP.[54] This is evidenced by the buried surface areas of IL-1RAcP D2 of 923 Å^2 and IL-1RAcP D3 of 754 Å^2 to the IL-33/ST2 surface.[45] This increase in buried surface area of IL-33/ST2 to IL-1RAcP D3 relative to that of IL-1 β/IL-1RI is due to a 60° rotation of IL-1RAcP D3 between the IL-1β- and IL-33-mediated ternary complexes, which exposes a larger side of the Ig domain for complex formation available for binding to the IL-33 and ST2 D3 (Figure 7B).[54] As Ig domains are ellipsoidal, IL-1β signaling comparatively uses a much narrower side of the IL-1RAcP D3, resulting in a buried surface area of 354 Å^2 made to the IL-1/IL-RI composite surface (Figure 7C). Altogether, IL-1β signaling utilizes a different stretch of residues in IL-1RAcP D3, S283–T291, for complex formation, with R286 alone contributing 2 kcal/mol energy to IL-1β-mediated complex formation.[54] In IL-33-mediated complex formation, this interaction with IL-1RAcP D3 is shifted to residues V221–V232, with V221 of IL-1RAcP contributing approximately 2 kcal/mol, V224 0.25 kcal/mol, V226 nearly 2 kcal/mol, and Y249 nearly 4 kcal/mol to IL-33 complex formation.[54]

Here, we found that CAN10 potently blocks IL-1, IL-33, and IL-36 signaling pathways by binding the c2d2 loop of IL-1RAcP, which is highly important for all IL-1RAcP-associated signaling (Figures 2, 4A, 4B, 6A, and 6B). Consequently, targeting an area known for its energetic contributions to all known IL-1 family signaling complexes provides a viable therapeutic strategy for broadly blocking all associated cytokine signaling from a shared receptor (Figure 2). 3G5, by a completely distinct mechanism, functions by sterically hindering two distinct regions of IL-1RAcP D3 that are important for both IL-1- and IL-33-mediated complex formation and signal transduction (Figure 7F). Strikingly, the potencies of CAN10 and 3G5 as inhibitors to IL-1RAcP-associated cytokines were remarkably similar in all instances despite their differing epitopes (Figures 2C–2H).

While our studies describe the mechanisms by which the two anti-IL-1RAcP mAbs CAN10 and 3G5 block all IL-1 cytokines that utilize this shared co-receptor, they highlight the need for future studies directed at IL-1RAcP usage by member cytokine complexes. While IL-1α and IL-1β share the same primary receptor, IL-1RI, they contain only 25% sequence homology. Do key interactions with IL-1RAcP differ between these distinct cytokines, and could these differences potentially be exploited for IL-1 cytokine isotype-specific

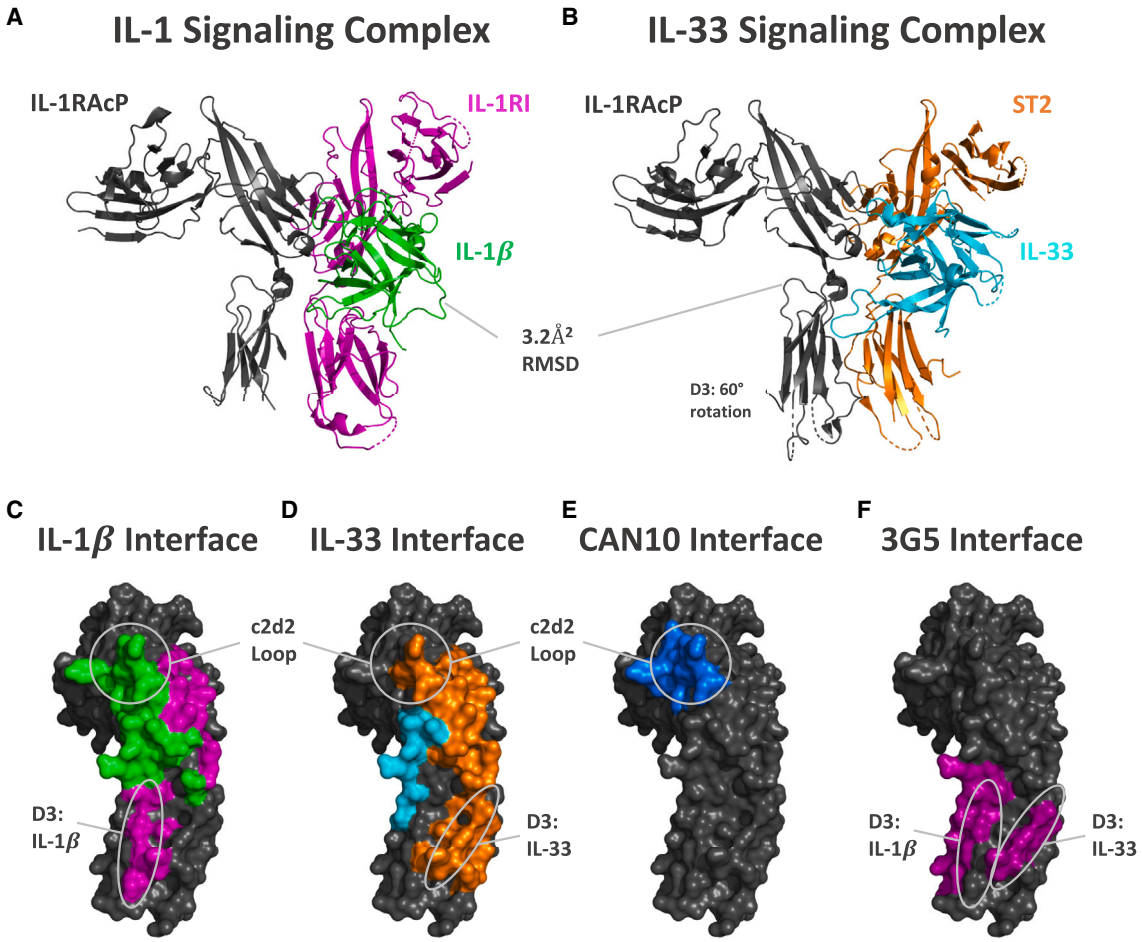

Figure 7. Structural analyses of known signaling complexes yield a rationale for broad signaling blockade

(A) Crystal structure of the IL-1β signaling complex (PDB: 4DEP), with receptors and cytokines labeled.

(B) Crystal structure of the IL-33 signaling complex (PDB: 5VI4), with receptors and cytokines labeled.

(C) Crystal structure of IL-1RAcP (PDB: 4DEP), with IL-1 (green) and IL-1RI (magenta) interfaces colored.

(D) Crystal structure of IL-1RAcP (PDB: 4DEP), with IL-33 (teal) and ST2 (orange) interfaces colored from the IL-33 complex (PDB: 5VI4).

(E) Crystal structure of IL-1RAcP (PDB: 4DEP), with the CAN10 interface (blue) colored from HDX-MS and SPR data.

(F) Crystal structure of IL-1RAcP (PDB: 4DEP), with the 3G5 interface (purple) colored from HDX-MS and SPR data.

blockade? Initial cytokine signaling inhibition with IL-1Ra, CAN10, and 3G5 would suggest this to be so, as the inhibitory capacity of IL-1Ra is 4-fold greater in IL-1α than in IL-1β. In IL-36 signaling, is the recruitment of IL-1RAcP similar to IL-1 and IL-33, or is it an entirely distinct strategy? CAN10's inhibition of IL-36 cytokines demonstrates that D2 is highly important in IL-36 signaling, as is the case with IL-1 signaling. As D3 is utilized distinctly by IL-1 and IL-33 signaling complexes, however, it is not possible to say for certain whether IL-36 signaling resembles IL-1, IL-33, or an entirely new usage of this highly variable domain. Nonetheless, targeting the shared co-receptor for IL-1, IL-33, and IL-36 cytokines, as with the anti-IL-1RacP-blocking antibodies CAN10 and 3G5, holds promise for the effective treatment of inflammatory and fibrotic diseases with benefits beyond inhibiting signaling by individual IL-1-family cytokines.

Limitations of the study

To date, a high-resolution structure of an IL-36 signaling complex (i.e., cytokine/primary receptor/secondary receptor) has not been determined. Therefore, we had to infer the mechanism of action of CAN10 inhibiting IL-36 cytokine signaling from previous experimental data involving comprehensive loop swaps of IL-36 agonist and antagonist cytokines.[61] While these data were highly beneficial for hypothesis generation for CAN10's mechanism of action, these studies were not able to shed light on how 3G5 inhibits IL-36 signaling. Indeed, as 3G5 has a broad epitope on IL-1RAcP that encompasses areas utilized by both IL-1 and IL-33 signaling complexes, we cannot state whether IL-36 signaling resembles IL-1 or IL-33 signaling in D3 utilization or, quite possibly, an entirely new utilization of D3. Regardless, our signaling data clearly show that 3G5 potently inhibits all IL-36 signaling.

STAR★METHODS

Detailed methods are provided in the online version of this paper and include the following:

- KEY RESOURCES TABLE
- RESOURCE AVAILABILITY
  - Lead contact
  - Materials availability
  - Data and code availability
- EXPERIMENTAL MODEL AND STUDY PARTICIPANT DETAILS
  - Mice
  - Cell lines
- METHOD DETAILS
  - Protein expression and purification
  - Generation of CAN10, 3G5, and mCAN10
  - mCAN10 binding data
  - In-vivo model of monosodium urate crystal (MSU) induced peritonitis
  - Surface plasmon resonance
  - Cell signaling assays
  - Chimeric IL-1RAcP ELISA
  - Hydrogen deuterium exchange coupled to mass spectrometry
  - Fab visualization
  - Alanine scanning mutagenesis
- QUANTIFICATION AND STATISTICAL ANALYSIS
  - Additional resources

SUPPLEMENTAL INFORMATION

Supplemental information can be found online at https://doi.org/10.1016/j.celrep.2024.114099.

ACKNOWLEDGMENTS

This work was supported by NIH grant AI132766 (to E.J.S.).

AUTHOR CONTRIBUTIONS

Study conception and design, J.K.F. and E.J.S.; acquisition of data, J.K.F., E.J.G., M.B., J.O., G.S.B., K.S., K.M., C.G., S.R., N.H., and T.F.; analysis and interpretation of data, J.K.F., E.J.G., M.B., G.S.B., K.S., C.G., S.R., N.H., T.F., D.D., and E.J.S.; drafting of manuscript, J.K.F. and E.J.S.; critical revision and editing, J.K.F., E.J.G., D.L., D.D., and E.J.S.; provision of key materials, M.B., K.M., K.K., M.F., A.K.S., and C.H.

DECLARATION OF INTERESTS

E.J.G., G.S.B., C.G., S.R., and D.L. are employees of Cantargia AB (Medicon Village, Lund, Sweden). K.S. is an employee of Innovagen AB (Lund, Sweden). E.J.G, G.S.B., K.S., C.G., S.R., T.F., and D.L. are shareholders of Cantargia AB. Cantargia AB is the owner of the intellectual property rights for CAN10 and 3G5 for use in the treatment of autoinflammatory and autoimmune diseases.

Received: October 17, 2023
Revised: February 24, 2024
Accepted: March 27, 2024
Published: April 17, 2024

REFERENCES

1. Dinarello, C.A., Simon, A., and van der Meer, J.W.M. (2012). Treating inflammation by blocking interleukin-1 in a broad spectrum of diseases. Nat. Rev. Drug Discov. *11*, 633–652. https://doi.org/10.1038/nrd3800.
2. Bresnihan, B., Alvaro-Gracia, J.M., Cobby, M., Doherty, M., Domljan, Z., Emery, P., Nuki, G., Pavelka, K., Rau, R., Rozman, B., et al. (1998). Treatment of rheumatoid arthritis with recombinant human interleukin-1 receptor antagonist. Arthritis Rheum. *41*, 2196–2204. https://doi.org/10.1002/1529-0131(199812)41:12<2196::AID-ART15>3.0.CO;2-2.
3. Larsen, C.M., Faulenbach, M., Vaag, A., Ehses, J.A., Donath, M.Y., and Mandrup-Poulsen, T. (2009). Sustained effects of interleukin-1 receptor antagonist treatment in type 2 diabetes. Diabetes Care *32*, 1663–1668. https://doi.org/10.2337/dc09-0533.
4. Ridker, P.M., Everett, B.M., Thuren, T., MacFadyen, J.G., Chang, W.H., Ballantyne, C., Fonseca, F., Nicolau, J., Koenig, W., Anker, S.D., et al. (2017). Antiinflammatory Therapy with Canakinumab for Atherosclerotic Disease. N. Engl. J. Med. *377*, 1119–1131. https://doi.org/10.1056/NEJMoa1707914.
5. Klein, A.L., Imazio, M., Cremer, P., Brucato, A., Abbate, A., Fang, F., Insalaco, A., LeWinter, M., Lewis, B.S., Lin, D., et al. (2021). Phase 3 Trial of Interleukin-1 Trap Rilonacept in Recurrent Pericarditis. N. Engl. J. Med. *384*, 31–41. https://doi.org/10.1056/NEJMoa2027892.
6. Pascual, V., Allantaz, F., Arce, E., Punaro, M., and Banchereau, J. (2005). Role of interleukin-1 (IL-1) in the pathogenesis of systemic onset juvenile idiopathic arthritis and clinical response to IL-1 blockade. J. Exp. Med. *201*, 1479–1486. https://doi.org/10.1084/jem.20050473.
7. Monaco, C., Nanchahal, J., Taylor, P., and Feldmann, M. (2015). Anti-TNF therapy: past, present and future. Int. Immunol. *27*, 55–62. https://doi.org/10.1093/intimm/dxu102.
8. Ruperto, N., Lovell, D.J., Quartier, P., Paz, E., Rubio-Pérez, N., Silva, C.A., Abud-Mendoza, C., Burgos-Vargas, R., Gerloni, V., Melo-Gomes, J.A., et al. (2010). Long-term safety and efficacy of abatacept in children with juvenile idiopathic arthritis. Arthritis Rheum. *62*, 1792–1802. https://doi.org/10.1002/art.27431.
9. Maini, R.N., Breedveld, F.C., Kalden, J.R., Smolen, J.S., Davis, D., Macfarlane, J.D., Antoni, C., Leeb, B., Elliott, M.J., Woody, J.N., et al. (1998). Therapeutic efficacy of multiple intravenous infusions of anti-tumor necrosis factor alpha monoclonal antibody combined with low-dose weekly methotrexate in rheumatoid arthritis. Arthritis Rheum. *41*, 1552–1563. https://doi.org/10.1002/1529-0131(199809)41:9<1552::AID-ART5>3.0.CO;2-W.
10. Weinblatt, M.E., Kremer, J.M., Bankhurst, A.D., Bulpitt, K.J., Fleischmann, R.M., Fox, R.I., Jackson, C.G., Lange, M., and Burge, D.J. (1999). A trial of etanercept, a recombinant tumor necrosis factor receptor:Fc fusion protein, in patients with rheumatoid arthritis receiving methotrexate. N. Engl. J. Med. *340*, 253–259. https://doi.org/10.1056/NEJM199901283400401.
11. Weinblatt, M.E., Keystone, E.C., Furst, D.E., Moreland, L.W., Weisman, M.H., Birbara, C.A., Teoh, L.A., Fischkoff, S.A., and Chartash, E.K. (2003). Adalimumab, a fully human anti-tumor necrosis factor alpha monoclonal antibody, for the treatment of rheumatoid arthritis in patients taking concomitant methotrexate: the ARMADA trial. Arthritis Rheum. *48*, 35–45. https://doi.org/10.1002/art.10697.
12. Choy, E.H., De Benedetti, F., Takeuchi, T., Hashizume, M., John, M.R., and Kishimoto, T. (2020). Translating IL-6 biology into effective treatments. Nat. Rev. Rheumatol. *16*, 335–345. https://doi.org/10.1038/s41584-020-0419-z.
13. Choy, E.H.S., Isenberg, D.A., Garrood, T., Farrow, S., Ioannou, Y., Bird, H., Cheung, N., Williams, B., Hazleman, B., Price, R., et al. (2002). Therapeutic benefit of blocking interleukin-6 activity with an anti-interleukin-6 receptor monoclonal antibody in rheumatoid arthritis: a randomized, double-blind, placebo-controlled, dose-escalation trial. Arthritis Rheum. *46*, 3143–3150. https://doi.org/10.1002/art.10623.

14. Tanaka, T., Hishitani, Y., and Ogata, A. (2014). Monoclonal antibodies in rheumatoid arthritis: comparative effectiveness of tocilizumab with tumor necrosis factor inhibitors. Biologics. *8*, 141–153. https://doi.org/10.2147/BTT.S37509.

15. De Benedetti, F., Brunner, H.I., Ruperto, N., Kenwright, A., Wright, S., Calvo, I., Cuttica, R., Ravelli, A., Schneider, R., Woo, P., et al. (2012). Randomized trial of tocilizumab in systemic juvenile idiopathic arthritis. N. Engl. J. Med. *367*, 2385–2395. https://doi.org/10.1056/NEJMoa1112802.

16. Ozaki, K., and Leonard, W.J. (2002). Cytokine and cytokine receptor pleiotropy and redundancy. J. Biol. Chem. *277*, 29355–29358. https://doi.org/10.1074/jbc.R200003200.

17. Dinarello, C.A. (2013). Overview of the interleukin-1 family of ligands and receptors. Semin. Immunol. *25*, 389–393. https://doi.org/10.1016/j.smim.2013.10.001.

18. Boraschi, D., and Tagliabue, A. (2013). The interleukin-1 receptor family. Semin. Immunol. *25*, 394–407. https://doi.org/10.1016/j.smim.2013.10.023.

19. Fields, J.K., Günther, S., and Sundberg, E.J. (2019). Structural Basis of IL-1 Family Cytokine Signaling. Front. Immunol. *10*, 1412. https://doi.org/10.3389/fimmu.2019.01412.

20. Robbrecht, D., Jungels, C., Sorensen, M.M., Spanggaard, I., Eskens, F., Fretland, S.Ø., Guren, T.K., Aftimos, P., Liberg, D., Svedman, C., et al. (2022). First-in-human phase 1 dose-escalation study of CAN04, a first-in-class interleukin-1 receptor accessory protein (IL1RAP) antibody in patients with solid tumours. Br. J. Cancer *126*, 1010–1017. https://doi.org/10.1038/s41416-021-01657-7.

21. Rydberg Millrud, C., Deronic, A., Grönberg, C., Jaensson Gyllenbäck, E., von Wachenfeldt, K., Forsberg, G., and Liberg, D. (2023). Blockade of IL-1alpha and IL-1beta signaling by the anti-IL1RAP antibody nadunolimab (CAN04) mediates synergistic anti-tumor efficacy with chemotherapy. Cancer Immunol. Immunother. *72*, 667–678. https://doi.org/10.1007/s00262-022-03277-3.

22. Järås, M., Johnels, P., Hansen, N., Agerstam, H., Tsapogas, P., Rissler, M., Lassen, C., Olofsson, T., Bjerrum, O.W., Richter, J., and Fioretos, T. (2010). Isolation and killing of candidate chronic myeloid leukemia stem cells by antibody targeting of IL-1 receptor accessory protein. Proc. Natl. Acad. Sci. USA *107*, 16280–16285. https://doi.org/10.1073/pnas.1004408107.

23. Barreyro, L., Will, B., Bartholdy, B., Zhou, L., Todorova, T.I., Stanley, R.F., Ben-Neriah, S., Montagna, C., Parekh, S., Pellagatti, A., et al. (2012). Over-expression of IL-1 receptor accessory protein in stem and progenitor cells and outcome correlation in AML and MDS. Blood *120*, 1290–1298. https://doi.org/10.1182/blood-2012-01-404699.

24. Ågerstam, H., Karlsson, C., Hansen, N., Sandén, C., Askmyr, M., von Palffy, S., Högberg, C., Rissler, M., Wunderlich, M., Juliusson, G., et al. (2015). Antibodies targeting human IL1RAP (IL1R3) show therapeutic effects in xenograft models of acute myeloid leukemia. Proc. Natl. Acad. Sci. USA *112*, 10786–10791. https://doi.org/10.1073/pnas.1422749112.

25. Ågerstam, H., Hansen, N., von Palffy, S., Sandén, C., Reckzeh, K., Karlsson, C., Lilljebjörn, H., Landberg, N., Askmyr, M., Högberg, C., et al. (2016). IL1RAP antibodies block IL-1-induced expansion of candidate CML stem cells and mediate cell killing in xenograft models. Blood *128*, 2683–2693. https://doi.org/10.1182/blood-2015-11-679985.

26. Dinarello, C.A. (2018). Overview of the IL-1 family in innate inflammation and acquired immunity. Immunol. Rev. *281*, 8–27. https://doi.org/10.1111/imr.12621.

27. Cayrol, C., and Girard, J.P. (2018). Interleukin-33 (IL-33): A nuclear cytokine from the IL-1 family. Immunol. Rev. *281*, 154–168. https://doi.org/10.1111/imr.12619.

28. Vigne, S., Palmer, G., Martin, P., Lamacchia, C., Strebel, D., Rodriguez, E., Olleros, M.L., Vesin, D., Garcia, I., Ronchi, F., et al. (2012). IL-36 signaling amplifies Th1 responses by enhancing proliferation and Th1 polarization of naive CD4+ T cells. Blood *120*, 3478–3487. https://doi.org/10.1182/blood-2012-06-439026.

29. Murakami-Satsutani, N., Ito, T., Nakanishi, T., Inagaki, N., Tanaka, A., Vien, P.T.X., Kibata, K., Inaba, M., and Nomura, S. (2014). IL-33 promotes the induction and maintenance of Th2 immune responses by enhancing the function of OX40 ligand. Allergol. Int. *63*, 443–455. https://doi.org/10.2332/allergolint.13-OA-0672.

30. Verma, A.H., Zafar, H., Ponde, N.O., Hepworth, O.W., Sihra, D., Aggor, F.E.Y., Ainscough, J.S., Ho, J., Richardson, J.P., Coleman, B.M., et al. (2018). IL-36 and IL-1/IL-17 Drive Immunity to Oral Candidiasis via Parallel Mechanisms. J. Immunol. *201*, 627–634. https://doi.org/10.4049/jimmunol.1800515.

31. Johnston, A., Xing, X., Wolterink, L., Barnes, D.H., Yin, Z., Reingold, L., Kahlenberg, J.M., Harms, P.W., and Gudjonsson, J.E. (2017). IL-1 and IL-36 are dominant cytokines in generalized pustular psoriasis. J. Allergy Clin. Immunol. *140*, 109–120. https://doi.org/10.1016/j.jaci.2016.08.056.

32. Cai, Y., Xue, F., Quan, C., Qu, M., Liu, N., Zhang, Y., Fleming, C., Hu, X., Zhang, H.G., Weichselbaum, R., et al. (2019). A Critical Role of the IL-1beta-IL-1R Signaling Pathway in Skin Inflammation and Psoriasis Pathogenesis. J. Invest. Dermatol. *139*, 146–156. https://doi.org/10.1016/j.jid.2018.07.025.

33. Blumberg, H., Dinh, H., Dean, C., Jr., Trueblood, E.S., Bailey, K., Shows, D., Bhagavathula, N., Aslam, M.N., Varani, J., Towne, J.E., and Sims, J.E. (2010). IL-1RL2 and its ligands contribute to the cytokine network in psoriasis. J. Immunol. *185*, 4354–4362. https://doi.org/10.4049/jimmunol.1000313.

34. Blumberg, H., Dinh, H., Trueblood, E.S., Pretorius, J., Kugler, D., Weng, N., Kanaly, S.T., Towne, J.E., Willis, C.R., Kuechle, M.K., et al. (2007). Opposing activities of two novel members of the IL-1 ligand family regulate skin inflammation. J. Exp. Med. *204*, 2603–2614. https://doi.org/10.1084/jem.20070157.

35. Marrakchi, S., Guigue, P., Renshaw, B.R., Puel, A., Pei, X.Y., Fraitag, S., Zribi, J., Bal, E., Cluzeau, C., Chrabieh, M., et al. (2011). Interleukin-36-receptor antagonist deficiency and generalized pustular psoriasis. N. Engl. J. Med. *365*, 620–628. https://doi.org/10.1056/NEJMoa1013068.

36. Renne, J., Schäfer, V., Werfel, T., and Wittmann, M. (2010). Interleukin-1 from epithelial cells fosters T cell-dependent skin inflammation. Br. J. Dermatol. *162*, 1198–1205. https://doi.org/10.1111/j.1365-2133.2010.09662.x.

37. Pauwels, N.S., Bracke, K.R., Dupont, L.L., Van Pottelberge, G.R., Provoost, S., Vanden Berghe, T., Vandenabeele, P., Lambrecht, B.N., Joos, G.F., and Brusselle, G.G. (2011). Role of IL-1alpha and the Nlrp3/caspase-1/IL-1beta axis in cigarette smoke-induced pulmonary inflammation and COPD. Eur. Respir. J. *38*, 1019–1028. https://doi.org/10.1183/09031936.00158110.

38. Botelho, F.M., Bauer, C.M.T., Finch, D., Nikota, J.K., Zavitz, C.C.J., Kelly, A., Lambert, K.N., Piper, S., Foster, M.L., Goldring, J.J.P., et al. (2011). IL-1alpha/IL-1R1 expression in chronic obstructive pulmonary disease and mechanistic relevance to smoke-induced neutrophilia in mice. PLoS One *6*, e28457. https://doi.org/10.1371/journal.pone.0028457.

39. Lappalainen, U., Whitsett, J.A., Wert, S.E., Tichelaar, J.W., and Bry, K. (2005). Interleukin-1beta causes pulmonary inflammation, emphysema, and airway remodeling in the adult murine lung. Am. J. Respir. Cell Mol. Biol. *32*, 311–318. https://doi.org/10.1165/rcmb.2004-0309OC.

40. Cayrol, C., and Girard, J.P. (2014). IL-33: an alarmin cytokine with crucial roles in innate immunity, inflammation and allergy. Curr. Opin. Immunol. *31*, 31–37. https://doi.org/10.1016/j.coi.2014.09.004.

41. Grotenboer, N.S., Ketelaar, M.E., Koppelman, G.H., and Nawijn, M.C. (2013). Decoding asthma: translating genetic variation in IL33 and IL1RL1 into disease pathophysiology. J. Allergy Clin. Immunol. *131*, 856–865. https://doi.org/10.1016/j.jaci.2012.11.028.

42. Torgerson, D.G., Ampleford, E.J., Chiu, G.Y., Gauderman, W.J., Gignoux, C.R., Graves, P.E., Himes, B.E., Levin, A.M., Mathias, R.A., Hancock, D.B., et al. (2011). Meta-analysis of genome-wide association studies of asthma

in ethnically diverse North American populations. Nat. Genet. *43*, 887–892. https://doi.org/10.1038/ng.888.

43. Sjöberg, L.C., Nilsson, A.Z., Lei, Y., Gregory, J.A., Adner, M., and Nilsson, G.P. (2017). Interleukin 33 exacerbates antigen driven airway hyperresponsiveness, inflammation and remodeling in a mouse model of asthma. Sci. Rep. *7*, 4219. https://doi.org/10.1038/s41598-017-03674-0.
44. Hojen, J.F., Kristensen, M.L.V., McKee, A.S., Wade, M.T., Azam, T., Lunding, L.P., de Graaf, D.M., Swartzwelter, B.J., Wegmann, M., Tolstrup, M., et al. (2019). IL-1R3 blockade broadly attenuates the functions of six members of the IL-1 family, revealing their contribution to models of disease. Nat. Immunol. *20*, 1138–1149. https://doi.org/10.1038/s41590-019-0467-1.
45. Fields, J.K., Kihn, K., Birkedal, G.S., Klontz, E.H., Sjöström, K., Günther, S., Beadenkopf, R., Forsberg, G., Liberg, D., Snyder, G.A., et al. (2021). Molecular Basis of Selective Cytokine Signaling Inhibition by Antibodies Targeting a Shared Receptor. Front. Immunol. *12*, 779100. https://doi.org/10.3389/fimmu.2021.779100.
46. Martinon, F., Pétrilli, V., Mayor, A., Tardivel, A., and Tschopp, J. (2006). Gout-associated uric acid crystals activate the NALP3 inflammasome. Nature *440*, 237–241. https://doi.org/10.1038/nature04516.
47. Menzies-Gow, A., Ying, S., Sabroe, I., Stubbs, V.L., Soler, D., Williams, T.J., and Kay, A.B. (2002). Eotaxin (CCL11) and eotaxin-2 (CCL24) induce recruitment of eosinophils, basophils, neutrophils, and macrophages as well as features of early- and late-phase allergic reactions following cutaneous injection in human atopic and nonatopic volunteers. J. Immunol. *169*, 2712–2718. https://doi.org/10.4049/jimmunol.169.5.2712.
48. Takatsu, K. (2011). Interleukin-5 and IL-5 receptor in health and diseases. Proc. Jpn. Acad. Ser. B Phys. Biol. Sci. *87*, 463–485. https://doi.org/10.2183/pjab.87.463.
49. Rivers-Auty, J., Daniels, M.J.D., Colliver, I., Robertson, D.L., and Brough, D. (2018). Redefining the ancestral origins of the interleukin-1 superfamily. Nat. Commun. *9*, 1156. https://doi.org/10.1038/s41467-018-03362-1.
50. Oshikawa, K., Yanagisawa, K., Tominaga, S., and Sugiyama, Y. (2002). Expression and function of the ST2 gene in a murine model of allergic airway inflammation. Clin. Exp. Allergy *32*, 1520–1526. https://doi.org/10.1046/j.1365-2745.2002.01494.x.
51. Hayakawa, H., Hayakawa, M., Kume, A., and Tominaga, S.i. (2007). Soluble ST2 blocks interleukin-33 signaling in allergic airway inflammation. J. Biol. Chem. *282*, 26369–26380. https://doi.org/10.1074/jbc.M704916200.
52. Towne, J.E., Renshaw, B.R., Douangpanya, J., Lipsky, B.P., Shen, M., Gabel, C.A., and Sims, J.E. (2011). Interleukin-36 (IL-36) ligands require processing for full agonist (IL-36alpha, IL-36beta, and IL-36gamma) or antagonist (IL-36Ra) activity. J. Biol. Chem. *286*, 42594–42602. https://doi.org/10.1074/jbc.M111.267922.
53. Thomas, C., Bazan, J.F., and Garcia, K.C. (2012). Structure of the activating IL-1 receptor signaling complex. Nat. Struct. Mol. Biol. *19*, 455–457. https://doi.org/10.1038/nsmb.2260.
54. Günther, S., Deredge, D., Bowers, A.L., Luchini, A., Bonsor, D.A., Beadenkopf, R., Liotta, L., Wintrode, P.L., and Sundberg, E.J. (2017). IL-1 Family Cytokines Use Distinct Molecular Mechanisms to Signal through Their Shared Co-receptor. Immunity *47*, 510–523.e4. https://doi.org/10.1016/j.immuni.2017.08.004.
55. Wang, D., Zhang, S., Li, L., Liu, X., Mei, K., and Wang, X. (2010). Structural insights into the assembly and activation of IL-1beta with its receptors. Nat. Immunol. *11*, 905–911. https://doi.org/10.1038/ni.1925.
56. Dinarello, C.A. (2011). Interleukin-1 in the pathogenesis and treatment of inflammatory diseases. Blood *117*, 3720–3732. https://doi.org/10.1182/blood-2010-07-273417.
57. Garlanda, C., Dinarello, C.A., and Mantovani, A. (2013). The interleukin-1 family: back to the future. Immunity *39*, 1003–1018. https://doi.org/10.1016/j.immuni.2013.11.010.
58. Estrov, Z., Kurzrock, R., Estey, E., Wetzler, M., Ferrajoli, A., Harris, D., Blake, M., Gutterman, J.U., and Talpaz, M. (1992). Inhibition of acute myelogenous leukemia blast proliferation by interleukin-1 (IL-1) receptor antagonist and soluble IL-1 receptors. Blood *79*, 1938–1945.
59. Voronov, E., Shouval, D.S., Krelin, Y., Cagnano, E., Benharroch, D., Iwakura, Y., Dinarello, C.A., and Apte, R.N. (2003). IL-1 is required for tumor invasiveness and angiogenesis. Proc. Natl. Acad. Sci. USA *100*, 2645–2650. https://doi.org/10.1073/pnas.0437939100.
60. Wang, X., Lupardus, P., Laporte, S.L., and Garcia, K.C. (2009). Structural biology of shared cytokine receptors. Annu. Rev. Immunol. *27*, 29–60. https://doi.org/10.1146/annurev.immunol.24.021605.090616.
61. Günther, S., and Sundberg, E.J. (2014). Molecular determinants of agonist and antagonist signaling through the IL-36 receptor. J. Immunol. *193*, 921–930. https://doi.org/10.4049/jimmunol.1400538.
62. Vazquez-Lombardi, R., Nevoltris, D., Luthra, A., Schofield, P., Zimmermann, C., and Christ, D. (2018). Transient expression of human antibodies in mammalian cells. Nat. Protoc. *13*, 99–117. https://doi.org/10.1038/nprot.2017.126.
63. Kivi, G., Teesalu, K., Parik, J., Kontkar, E., Ustav, M., Jr., Noodla, L., Ustav, M., and Männik, A. (2016). HybriFree: a robust and rapid method for the development of monoclonal antibodies from different host species. BMC Biotechnol. *16*, 2. https://doi.org/10.1186/s12896-016-0232-6.
64. Kabsch, W. (2010). Xds. Acta Crystallogr. D Biol. Crystallogr. *66*, 125–132. https://doi.org/10.1107/S0907444909047337.
65. Evans, P.R., and Murshudov, G.N. (2013). How good are my data and what is the resolution? Acta Crystallogr. D Biol. Crystallogr. *69*, 1204–1214. https://doi.org/10.1107/S0907444913000061.
66. Vagin, A., and Teplyakov, A. (2010). Molecular replacement with MOLREP. Acta Crystallogr. D Biol. Crystallogr. *66*, 22–25. https://doi.org/10.1107/S0907444909042589.
67. Murshudov, G.N., Vagin, A.A., and Dodson, E.J. (1997). Refinement of macromolecular structures by the maximum-likelihood method. Acta Crystallogr. D Biol. Crystallogr. *53*, 240–255. https://doi.org/10.1107/S0907444996012255.
68. Emsley, P., Lohkamp, B., Scott, W.G., and Cowtan, K. (2010). Features and development of Coot. Acta Crystallogr. D Biol. Crystallogr. *66*, 486–501. https://doi.org/10.1107/S0907444910007493.
69. Leem, J., Dunbar, J., Georges, G., Shi, J., and Deane, C.M. (2016). ABodyBuilder: Automated antibody structure prediction with data-driven accuracy estimation. mAbs *8*, 1259–1268. https://doi.org/10.1080/19420862.2016.1205773.

STAR★METHODS

KEY RESOURCES TABLE

REAGENT or RESOURCE	SOURCE	IDENTIFIER
Antibodies		
mCAN10	Cantargia AB	NA
CAN10	Cantargia AB	NA
3G5	Cantargia AB	NA
anti-HEL mIgG2a-LALA-PG	Icosagen	NA
Bacterial and virus strains		
Bacteria: *E. Coli* Top10	Sundberg Lab	NA
Bacteria: *E. Coli* BL21 DE3	Sundberg Lab	NA
Bacteria: *E. Coli* DH5 α	Icosagen	NA
Lipofectamine	Thermofisher	L3000001
Puromycin	Invivogen	ant-pr-1
Biological samples		
No biological samples were used in this study	NA	NA
Chemicals, peptides, and recombinant proteins		
Mono-sodium urate crystals	Invivogen	MSU-42-01
Index Screen (crystallography screen)	Hampton Research	HR2-144
Kineret (Anakinra/IL-1Ra)	Sobi, Sweden	NA
sST2 (human)	RnD Systems	523-ST
IL-36Ra (human)	RnD Systems	1275-IL/CF
IL-1 α (human)	Peprotech	200-01A
IL-1 β (human)	Peprotech	200-01B
IL-33 (human)	Peprotech	200–33
IL-36 α (human)	RnD Systems	6995-IL-010
IL-36 β (human)	RnD Systems	6834-ILB-025
IL-36 γ (human)	RnD Systems	6835-IL-010
IL-1 α (murine)	RnD Systems	400-ML-005
IL-1 β (murine)	RnD Systems	401-ML-005
IL-33 (murine)	Peprotech	210–33
IL-36 α (murine)	RnD Systems	1059-ML-010
IL-36 β (murine)	RnD Systems	7060-ML-010
IL-36 γ (murine)	RnD Systems	6996-IL-010
Protein A from *S. Aureus*	Sigma Aldrich	P7837-5MG
Critical commercial assays		
Multiplex immunoassay (IL-6 from NIH3T3cells)	Eve Technologies	Mouse Cytokine 32-Plex Discovery Assay
Luminex (IL-6 and KC)	RnD	LXSAMSM-02
Luminex	BioRad	IL-5, Cat#: 171G5006M Eotaxin, Cat#: 171G5014M G-CSF, Cat#: 171G5015M MCP-1, Cat#: 171G5019M MIP-1b, Cat#: 171G5021M Plates, Cat#: 12002798 Standard, Cat#: 171I50001
Deposited data		
3G5 Crystal Structure	RCSB	PDB: 8VFU
Experimental models: Cell lines		
HEK-Blue™ IL-1/IL-33 cells	Invivogen	hkb-il33

(*Continued on next page*)

Continued		
REAGENT or RESOURCE	SOURCE	IDENTIFIER
HEK-Blue™ cells, IL36R transfected	Cantargia AB	NA
HEK-293T cells	ATCC	CRL-3216
NIH3T3cells	ATCC	CRL-1658
Experimental models: Organisms/strains		
IL-1RAcP KO and WT littermate mice: B6; 129S1-Il1raptm1Roml/J strain	Thoas Fioretos Lab	Strain #003284; RRID: IMSR_JAX003284
C57/Bl6	Taconic	C57BL/6NTac
Oligonucleotides		
No oligonucleotides were used in this study	NA	NA
Recombinant DNA		
CAN10 Fab (Heavy and Light Chains) pcDNA3.1	Sundberg Lab	NA
3G5Fab (Heavy and Light Chains) pcDNA3.1	Sundberg Lab	NA
IL-1 α pet30a	Sundberg Lab	NA
IL-1 β pet30a	Sundberg Lab	NA
IL-33 pet28a	Sundberg Lab	NA
IL-36 α pet30a	Sundberg Lab	NA
IL-36 β pet30a	Sundberg Lab	NA
IL-36 γ pet30a	Sundberg Lab	NA
IL-1RAcP pcDNA4/TO	Sundberg Lab	NA
IL-1RAcP domain 1/2 pcDNA4/TO	Sundberg Lab	NA
IL-1RAcP domain 3 pcDNA4/TO	Sundberg Lab	NA
IL-1RAcP Fc-fusion pcDNA4/TO	Sundberg Lab	NA
IL36R construct (Uniprot Q9HB29)	Cantargia AB	NA
Software and algorithms		
Dynamx 3.0	Waters	NA
Pymol	Schrödinger	NA
CCP4 (Version 8.0)	Collaborative Computational Project No. 4	NA
Phenix (Version 1.2)	Phenix	NA
Biacore Evaluation Software (T100)	Cytiva	NA
FlowJo	BD Life Sciences	NA
Graph Pad PRISM	GraphPad Prism for Windows, GraphPad Software, Boston, Massachusetts USA, www.graphpad.com	NA
Other		
No other materials were used in this study	NA	NA

RESOURCE AVAILABILITY

Lead contact

Further information and requests for resources and reagents should be directed to and will be fulfilled by the lead contact, Eric J. Sundberg, PhD (eric.sundberg@emory.edu).

Materials availability

Plasmids used in this study are available upon request from the lead contact.

Data and code availability

- The data supporting the findings of this study are available within the article and its supplementary figures. In addition, data reported in this paper can be shared by the lead contact upon request. The reported crystal structure of 3G5 can be accessed through the RCSB (pdb: 8VFU).
- This paper does not report original code.
- Any additional information required to reanalyze the data reported in this work paper is available from the lead contact upon request.

EXPERIMENTAL MODEL AND STUDY PARTICIPANT DETAILS

Mice

Mice used in this study: 8–9 weeks old female C57Bl/6 mice were used for the testing of mCAN10, anti-HEL isotype control, and IL-1Ra control experiments in MSU challenge (Figures 1B–1D). In the preceding experiment (Figure 1A), 12–20 weeks old male and female wild type C57Bl/6 mice, or IL-1RAcP KO littermate mice from the B6; 129S1-*Il1rap*^{tm1Roml}/J strain (Strain #:003284, RRID: IMSR_JAX:003284) back crossed to a C57Bl/6 background, were used. Animal experiments were performed at Truly Labs AB (Lund Sweden) and approved by the local ethics committee (ethical permit (5.8.18–10848/2017)).

Cell lines

Cell signaling assays

In Figure 2, HEK-Blue IL-1/IL-33 cells (Invivogen: Cat #hkb-il33) or HEK-Blue IL-1/IL-33 cells stably transfected in house with human IL36R, within referred to as HEK-Blue IL36R cells, were used. These cells were growing in DMEM with 4.5 g/L glucose, 2 mM L-glutamine, 10% (v/v) heat-inactivated fetal bovine serum, 100 U/ml penicillin, 100 μg/mL streptomycin, 100 μg/mL Normocin at 37*C with 5% CO_2. In Figure S8, HEK293T cells, grown in in freestyle media supplemented with glutamax (1/100) at 37*C, were transiently transfected with a luciferase reporter.

Eukaryotic expression

To express IL-1RAcP and its variants, HEK293T cells were transiently transfected in freestyle media supplemented with glutamax (1/100); CAN10 and 3G5 Fabs were also expressed using HEK293T cells. For the expression of the full length CAN10 and 3G5 mAbs, HEK293F, again grown in freestyle media, were transiently transfected.

METHOD DETAILS

Protein expression and purification

IL-1RAcP, cloned in a pcDNA4TO vector, was expressed in HEK293T cells and purified by nickel affinity chromatography and gel filtrated on a Superdex200 column; in its deglycosylated form, IL-1RAcP was expressed in HEK293 media supplemented with kifunesine (1ug/mL) to create a high-mannose variant glycan chains that were subsequently cleaved with the Endoglycosidase A (EndoA) prior to purification.[54,45] CAN10 and 3G5 mAbs were produced by transient gene expression in HEK293F cells as human immunoglobulin 1 (hIgG1) with Fc-silent "LALA" mutations [46,47]. Next, cell culture media was harvested and mAbs were purified by Protein A chromatography (mAbSelect SuRe, Cytiva). These mAbs were further purified by size exclusion chromatography on a Superdex200 column (GE Healthcare) equilibrated with 20mM HEPES, 150mM NaCl, pH 7.4 buffer. CAN10 and 3G5 Fabs were cloned into previously described Fab backgrounds in pcDNA3.1 plasmids and co-expressed in HEK293T cells prior to purification by nickel affinity chromatography and gel filtration on a Superdex200 column with 20mM HEPES, 150mM NaCl, pH 7.4 buffer.[62]

Generation of CAN10, 3G5, and mCAN10

CAN10 was generated by immunization of rabbits with a mixture of recombinantly expressed ectodomains of human and murine IL-1RAcP. After boosting, spleens were collected, homogenized, and monoclonal antibody sequences were isolated from immunized rabbits.[63] Streptavidin coated 96-well plates were coated with biotinylated human or murine IL-1RAcP, or a mixture of both. After incubation with spleen cells, coated wells were washed with PBS to remove unbound cells. RNA was isolated from the bound cells and VH and VL cDNA was synthesized and used for construction of a combinatorial VH-VL library in a human IgG expression plasmid format. Plasmid DNA was purified and transfected into CHO cells for production of chimeric rabbit/human IgG1 pools. Supernatants of antibody pools were analyzed using ELISA and positive pools were identified. Bacteria containing plasmid DNA from the positive pools were plated on LB-ampicillin solid medium and single colonies were isolated and grown in liquid medium. Plasmid DNA was purified from the liquid cultures and transfected into CHO cells for transient antibody production and identification of antibodies binding to human IL-1RAcP. The chimeric rabbit/human IgG1 ELISA IL-1RAcP positive clones were then analyzed for their properties, such as the ability to inhibit IL-1, IL-33 or IL-36 signaling. Selected clones were further characterized and humanized, resulting in generation of the mAb CAN10.

3G5 was generated by immunization of mice with human IL-1RAcP. After humanization, hybridomas were generated and the supernatants from growing hybridomas were screened with ELISA where the specific antibody titer was measured by coating plates

with human IL-1RAcP. Unique human IL-1RAcP mAbs identified were then further analyzed in their properties, such as the ability to inhibit IL-1, IL-33 or IL-36 signaling, and 3G5 was chosen for further studies.

To generate mCAN10, a murine IL-1RAcP binding signaling blocking surrogate, chickens were immunized with mouse IL-1RAcP protein, three times after every 2–2.5 weeks, and boosted twice, whereafter spleens were isolated, homogenized and subjected to monoclonal antibody development using the HybriFree technology described in Kivi *et al.*[63] Briefly, Immuno modules (Thermo Scientific) were coated with antigen and panning reactions performed. After incubation, wells were washed with PBS to remove the unbound cells and RNA was isolated and cDNA was synthesized using SuperScript III First-Strand Synthesis System for RT-PCR (Invitrogen) and used for VH and VL amplification. Amplified VH and VL were then purified and circular polymerase extension cloning (CPEC) reactions were performed for scFv-hFc expression vectors "pools" construction. E. coli DH5α was transformed by scFv-hFc expression vector pools and grown in liquid medium. Plasmid DNA was purified and transfected into CHOEBNALT85 cells for scFv-hFc pools production. Supernatants were analyzed by ELISA to identify antigen specific reaction, single clones were then selected in LB-Amp solid medium, and, lastly, grown in liquid medium in 96-well microtiter plate at 37*C. Next, plasmid DNA was isolated and transfected into CHOEBNALT85 cells for antibody transient production. Unique mouse IL-1RAcP mAbs identified were further analyzed in their properties, such as the ability to inhibit IL-1, IL-33 or IL-36 signaling and mCAN10 was chosen as the best functional surrogate for CAN10 due to its binding domain 2 and its ability to comprehensively inhibit all IL-1RAcP associated cytokines.

mCAN10 binding data

To specifically address which domain of IL-1RAcP contains critical epitopes for the CAN10 functional surrogate clone mCAN10, ELISA measurements using human IL-1RAcP, mouse IL-1RAcP and chimeric mouse/human IL-1RAcP constructs were performed with each chimeric variant of IL-1RAcP.[24] Briefly, microtiter plates were coated with mouse, human, or chimeric mouse/human IL-1RAcP and incubated overnight at 4°C. Subsequently, mCAN10 was added to the wells and, after extensive washing and blocking, the absorbance was measured at 405nm. Absorbance at 0 min was used as background signal.

In-vivo model of monosodium urate crystal (MSU) induced peritonitis

To induce inflammation, 2.5 mg monosodium urate crystals (MSU; InvivoGen MSU-42-01) were administered i.p. to 8–9 weeks old female C57Bl/6 mice to induce inflammation in the peritoneal cavity. Anti-mouse IL-1RAcP mCAN10 (20 mg/kg), anti-HEL mIgG2a-LALA-PG (isotype control; 20 mg/kg) or equimolar concentration of IL-1Ra (2.3 mg/kg; 133 nmol/kg, Anakinra, Sobi, Sweden) treatment was administered as an i.p. injection 1 h prior to MSU challenge. In a separate experiment, 12–20 weeks old male and female wild type, or IL-1RAcP KO littermate mice from the B6; 129S1-*Il1rap*^{tm1Roml}/J strain (Strain #:003284, RRID: IMSR_JAX:003284) back crossed to a C57Bl/6 background, were injected i.p. with 2.5 mg MSU. Six hours post MSU challenge, the animals were euthanized, and the peritoneal lavage was isolated to retrieve inflammatory cells and proteins from the peritoneal cavity. Immune cell counting and phenotyping were performed by flow cytometry (CytoFlex, Beckman Coulter) and cytokines in the peritoneal lavage were analyzed by Luminex (R&D systems or BioRad), according to the manufacturer's instructions. Animal experiments were performed at Truly Labs AB (Lund Sweden) and approved by the local ethics committee (ethical permit (5.8.18–10848/2017)).

Surface plasmon resonance

Affinities and kinetic parameters of protein-protein interactions were measured on a Biacore T100 biosensor (GE Healthcare) by surface plasmon resonance (SPR). 2000 response units (RU) of protein A from *Staphylococcus aureus* (Sigma Aldrich) were amine coupled on all flow channels of a CM5 sensor chip. Approximately 200 RU of CAN10 and 3G5 were captured directly on flow cell 2. IL-1RAcP and its variants were then used as the analyte and titrated over flow cells 1 and 2 in 2-fold dilutions, from 1.25nM to 20nM. Sensorgrams were double referenced against the control flow cell and buffer injections. Data were fit to a 1:1 binding model using Biacore T100 Evaluation software.

Cell signaling assays

Cell signaling assays for CAN10 and 3G5 were performed using HEK-Blue IL-1/IL-33 cells (Invivogen: Cat #hkb-il33) or HEK-Blue IL-1/IL-33 cells stably transfected in house with human IL36R, hereafter called HEK-Blue IL36R cells. For the generation of the stable HEK-Blue IL36R cells, a full length human IL36R construct carrying puromycin resistance was transfected into the HEK-Blue IL-1/IL-33 cells using Lipofectamine 3000 (ThermoFisher Scientific), and selection with increasing concentrations of puromycin (Invivogen) was carried out over 14 days. Expression of IL36R was confirmed with flow cytometry. HEK-Blue IL-1/IL-33 cells and HEK-Blue IL36R cells were cultured in complete medium (DMEM + Glutamax +10% full FBS + zeocin, normocin, hygromycin B gold and blasticidin). For measuring the inhibition of IL-1α, IL-1β, IL-33, and IL36-α/β/γ signaling, the appropriate HEK-Blue cells (9.5 x 10^3 cells/well) were seeded into 384-well plates and allowed to settle 2 h before continuing. Cells were then exposed to increasing concentrations of CAN10, 3G5, or antagonists (ST2, RnD Systems; IL-36Ra/IL-1F5, RnD Systems and IL-1Ra (Kineret/Anakinra, Sobi, Sweden) as indicated and incubated for 1 h at 37°C, 5% CO_2, before addition of each cytokine at the determined EC_{80} concentration (IL-1α 0.2 ng/mL, Peprotech; IL-1β 2 ng/ml, Peprotech; IL33 0.2 ng/mL, Peprotech; IL-36α 20 pg/mL, RnD Systems; IL-36β 14 pg/mL, RnD Systems; or IL-36 γ 5 pg/mL, RnD Systems). Cells were then cultured overnight (16–18 h) at 37°C, 5% CO_2 and analyzed for activation of NF-κB and subsequent production of SEAP using QUANTI-Blue solution measured at 620 nm using the SpectraMax i3x spectrophotometer.

Cell signaling assays for mCAN10 (Cantargia AB, Lund, Sweden), a monoclonal pan IL1/IL33/IL36 signaling blocking anti-mouse IL-1RAcP CAN10 surrogate mIgG2a antibody with L234A, L235A and P329G [LALA-PG] Fc-silencing mutations, were performed using the murine fibroblast cell line NIH3T3 (ATCC, CRL-1658). NIH3T3cells (4 x10^4 cells per well) were pre-incubated in a 96 well plate with anti-IL-1RAcP mCAN10 or isotype control antibodies as indicated (20 μg/ml for stimulation with IL-1 β, IL-33 and IL36 α/β/γ; 60 μg/mL for stimulation with IL-1α). After 60 min, cytokines were added: IL-1α (5 pg/mL, RnD Systems), IL-1β (30 pg/mL, RnD Systems), IL-33 (15 ng/mL, Peprotech) IL-36α (15 ng/mL, RnD Systems), IL-36β (8 ng/mL, RnD Systems) or IL-36γ (15 ng/mL, RnD Systems). Supernatants were then collected after 18 h of incubation at 37°C and analyzed for IL-6 cytokine release using multiplex immunoassay (Eve Technologies).

Cell signaling assays for possible synergism between CAN10 and 3G5 for Figure S8 were conducted in HEK293T cells. A luciferase reporter cassette downstream of an NF-κB promoter was transiently transfected into HEK293T cells.[45] Subsequently, these cells were pre-incubated with either CAN10, 3G5, or a 1:1 mixture of CAN10/3G5 from 1 μM to 1pm concentrations in a 96-well plate. After 30 min, these cells were stimulated with IL-1β and, after 5 h, were measured for luciferase activity by luminesce to determine the inhibitory capacities of these antibody mixtures.

Chimeric IL-1RAcP ELISA

The ELISA Measurements using chimeric IL-1RAcP constructs were performed with microtiter plates that were coated with mouse, human, or chimeric mouse/human IL-1RAcP and were subsequently incubated overnight at 4°C.[45] After extensive washing and blocking, a series of CAN10 dilutions were added to the wells. Polyclonal antibodies KMT-2 (affinity purified rabbit polyclonal antibodies against hIL-1RAcP) and KMT-3 (affinity purified rabbit polyclonal antibodies against mIL-1RAcP) were used as controls. Absorbance at 405 nm was then measured and absorbance at 0 min was used as background signal.

Hydrogen deuterium exchange coupled to mass spectrometry

In the hydrogen deuterium exchange mass spectrometry (HDX-MS) experiments, peptide identification and coverage maps for IL-1RAcP, CAN10, and 3G5 were obtained from undeuterated controls as follows: 1 μL of 20 μM protein in 20mM HEPES, 150mM NaCl, pH 7.4 was diluted with 19 μL ice-cold quench (50 mM Glycine pH 2.4, 8M Urea, 200mM TCEP) for 1 min prior to dilution with 180 μL 1XQ and injection into a Waters HDX technology system (Waters, Milford, MA) equipped with an M-Class UPLC and a Synapt G2Si mass spectrometer.[45] Peptides were identified using the ProteinLynx Global Server 3.0.3 (PLGS) from Waters. HDX reactions were conducted as follows for each protein and protein complex: 1 μL of 20 μM protein (apo or complex) was incubated with 9 μL 20 mM HEPES 99.99% D_2O, pH 7.4, 150 mM NaCl prior to quench at various times (10 s, 1 min,10 min, 2 h) with 50 μL of 50 mM Glycine pH 2.4, 8M Urea, 200mM TCEP 99.99% D_2O before dilution with 190 μL of 1XQ and ultimate injection. All deuteration time points were acquired in triplicate. Spectral curation, centroid calculation, and deuterium uptake for all identified peptides with increasing deuterium incubation time were performed using Water's DynamX 3.0 software.

Fab visualization

The Fab 3G5 was concentrated to 10-12 mg/mL and subjected to crystallization by vapor diffusion. Initially, crystals were observed in the Index Screen (Hampton Research) in 0.2M Trimethylamine N-oxide dihydrate, 0.1M Tris pH 8.5, and 20% w/v PEG. Larger crystals were grown in the same condition by hanging drop and cryo-protected with 25% w/v glycerol in mother liquid. A single dataset was collected at BNL NSLS-II Beamline 17-ID-1 (AMX). The dataset was processed using XDS[64] and Aimless,[65] with the initial phases being obtained by molecular replacement utilizing MOLREP,[66] with the light chain 6SVL and the heavy chain 5F3B as search models. The final model was built with iterative rounds of refinement with REFMAC[67] and Coot[68] and a final refinement with Phenix. The final model was deposited on the RCSB (PDB: 8VFU).

The Fab CAN10 was modeled using ABodyBuilder FV prediction[69] and is used purely for visualization of deuterium uptake changes in our corresponding HDX-MS experiments. As further validation of this modeling technique, the crystal structure 3G5 (pdb: 8VFU) was aligned to its predicted structure, again utilizing ABodyBuilder.[69] These two structures were highly similar, as reflected by an RMSD of 0.40 between their c α atoms.

Alanine scanning mutagenesis

Alanine scanning mutants were generated by site-directed mutagenesis (Qiagen) on Fc-fused IL-1RacP constructs; this library mirrored that of Gunther et al.[54] Briefly, kinetic parameters and affinities of protein-protein interactions were measured by SPR analysis on a Biacore T100 biosensor (GE Healthcare). 2000 response units of protein A from *staphylococcus aureus* (Sigma Aldrich) were amine coupled on all four flow channels of a CM5 sensor chip. Approximately 200 RU of Fc-fused IL-1RacP (IL-1RacP-Fc) were captured on flow channels 2, 3, or 4, with wild-type IL-1RacP-Fc being included in every experiment set as an internal standard. Binding experiments were carried out in 10mM HEPES, 150mM NaCl, 3mM EDTA, 0.005% (v/v) Tween 20 (HBS-EP) at 25C by single cycle kinetic analysis using five concentrations of CAN10 or 3G5 Fab, from 1.25nM to 20nM. For CAN10, N166A, F167A, and N168A mutations on IL-1RacP-Fc were repeated using 12.5nM–200nM of Fab (analyte) due to significantly decreased binding affinities; for 3G5, V224A, H226A, and Y249A mutations on IL-1RacP-Fc were repeated using 12.5nM–200nM of Fab for the above-mentioned reason.

Between runs, the sensor surface was regenerated using one injection of 10mM HCl. Sensorgrams were double referenced against control flow cell 1 and buffer injections. Data were fit to a 1:1 binding model using Biacore T100 evaluation software. All data points graphed are in triplicate.

QUANTIFICATION AND STATISTICAL ANALYSIS

In Figure 1A, the statistics above the bars show differences for total cells/mL between groups, while the statistics inside the bars show differences for neutrophils and monocytes specifically, between groups. Graph shows mean values. Statistical analysis was done using Mann-Whitney and defined as $^{*}p < 0.05$; $^{**}p < 0.01$; $^{***}p < 0.005$; $^{****}p < 0.001$. Here n means number of mice; WT ($n = 11$) and knockout (KO) ($n = 6$) mice. Statistical analysis was performed using GraphPad PRISM Software (V10.2).

In Figure 1C, statistical analysis was done using Mann-Whitney and defined as $^{*}p < 0.05$; $^{**}p < 0.01$; $^{***}p < 0.005$; $^{****}p < 0.001$. Each symbol represents one mouse. Line at mean. Here the n can be seen in the graph itself where each symbol represents one mouse (Ctrl $n = 4$, PBS $n = 6$, IL1RA $n = 8$, Isotype $n = 8$, mCAN10 $n = 8$). Statistical analysis was performed using GraphPad PRISM Software (V10.2).

In Figure 1D, cytokine profiles by Luminex from peritoneal lavage of the same mice as in 1C (as evident from Figure 1B). As the same mice were used in 1D as 1C, we have the same number of mice as in 1C (Ctrl $n = 4$, PBS $n = 6$, IL1RA $n = 8$, Isotype $n = 8$, mCAN10 $n = 8$). Graph shows mean and SEM. Statistical analysis was done using Mann-Whitney $^{*}p < 0.05$; $^{**}p < 0.01$; $^{***}p < 0.005$; $^{****}p < 0.001$. The statistics shown for mCAN10 vs. IL1Ra is normalized to vehicle and isotype controls, respectively. Statistics not shown: decrease in concentrations of analytes for IL1Ra and mCAN10 vs. their respective controls; G-CSF (IL1Ra vs. PBS ***; mCAN10 vs. iso ***); IL-6 (IL1Ra vs. PBS **; mCAN10 vs. iso **); IL-5 (IL1Ra vs. PBS *ns*; mCAN10 vs. iso *), Eotaxin (IL1Ra vs. PBS *ns*; mCAN10 vs. iso **); MIP1b (IL1Ra vs. PBS *ns*; mCAN10 vs. iso *); MCP1 (IL1Ra vs. PBS *ns*; mCAN10 vs. iso *) KC (IL1Ra vs. PBS *ns*; mCAN10 vs. iso *ns*). Statistical analysis was performed using GraphPad PRISM Software (V10.2).

For the cell signaling assays (Figures S1, 2, and S8), all data were obtained in triplicate and statistics were completed in GraphPad PRISM Software (V10.2).

For the HDX-MS experiments, Figures 4 and 5, data were obtained in triplicate. Both mean deuterium uptake and standard deviation were plotted on graphs and calculated in Microsoft excel (V16.83).

For the SPR alanine scan experiments, Figure 6, all data were obtained in triplicate. Mean ΔΔ G was plotted with standard deviation shown. These statistics were calculated in Microsoft excel (V16.83).

Additional resources

Description: URL to CAN10 clinical trial: A Study to Investigate the Safety and Tolerability of CAN10 Antibody in Healthy Subjects and in Subjects With Plaque Psoriasis. - Full Text View - ClinicalTrials.gov.